Assessing the global contribution of marine, terrestrial bioaerosols, and desert dust to ice-nucleating particle concentrations

Marios Chatziparaschos[1,2,*], Stelios Myriokefalitakis[3], Nikos Kalivitis[1], Nikos Daskalakis[4], Athanasios Nenes[2,5], María Gonçalves Ageitos[6,7], Montserrat Costa-Surós[6], Carlos Pérez García-Pando[6,8], Mihalis Vrekoussis[4,9,10] and Maria Kanakidou[1,2,4]

[1]Environmental Chemical Processes Laboratory (ECPL), Department of Chemistry, University of Crete, Heraklion
[2]Center for the Study of Air Quality and Climate Change (C-STACC), Institute of Chemical Engineering Sciences (ICE-HT), Foundation for Research and Technology, Hellas) (FORTH), Patras, Greece
[3]Institute for Environmental Research and Sustainable Development, National Observatory of Athens (NOA), GR-15236 Palea Penteli, Greece
[4]Laboratory for Modelling and Observation of the Earth System (LAMOS), Institute of Environmental Physics (IUP), University of Bremen, Bremen, Germany
[5]Laboratory of Atmospheric Processes and their Impacts (LAPI), School of Architecture, Civil and Environmental Engineering (ENAC), Ecole Polytechnique Federale de Lausanne, Lausanne, Switzerland
[6]Barcelona Supercomputing Center (BSC), Barcelona, Spain
[7]Department of Project and Construction Engineering, Universitat Politècnica de Catalunya (UPC), Barcelona, Spain
[8]Catalan Institution for Research and Advanced Studies (ICREA), Barcelona, Spain
[9]Center of Marine Environmental Sciences (MARUM), University of Bremen, Germany
[10]Climate and Atmosphere Research Center (CARE-C), The Cyprus Institute, Nicosia, Cyprus
*Now at Barcelona Supercomputing Center (BSC), Barcelona, Spain

Correspondence: Maria Kanakidou (mariak@uoc.gr)

Abstract. Aerosol-cloud interactions, and particularly ice ~~crystals~~processes in mixed-phase clouds (MPC), ~~stand as~~remain a key source of uncertainty in climate change assessments. ~~State~~This study introduces state-of-the-art laboratory-based parameterizations ~~were introduced~~ into a global chemistry-transport model to investigate the ~~contribution~~contributions of mineral dust~~,~~ (specifically K-feldspar and quartz), marine primary organic aerosol (MPOA), and terrestrial primary biological aerosol particles (PBAP) to ice nucleating particles (INP) in MPC. The model suggests that INP originating from PBAP (INP_{PBAP}) ~~are found to be~~is the primary source of INP at low altitudes between -10ºC and -20ºC, particularly in the tropics, with a pronounced peak in the Northern Hemisphere (NH) during the boreal summer. INP_{PBAP} contributes ~~about 27% (in the NH) and 30% (in the SH)~~over 40% of the total simulated INP ~~population.~~column burden at mid-latitudes. Dust-derived INP (INP_D) ~~show a~~is prominent ~~presence~~ at high altitudes ~~in~~across all seasons, dominating at temperatures below -~~25~~20°C, ~~constituting 68~~and constitutes over 89% of the INP average column burden~~. MPOA-derived INP (INP_{MPOA}) dominate~~ at high latitudes in the NH and about 74% at high latitudes in the Southern Hemisphere (SH~~),~~). MPOA-derived INP (INP_{MPOA}) prevails in the SH, particularly at subpolar and polar latitudes at low altitudes for temperatures ~~below -16ºC, representing approximately 46~~above -20ºC, where they represent between 17% and 36% of the INP column population ~~in~~, depending on

the ~~SH~~ season. When evaluated against available global observational INP data, the model achieves its highest predictability across all temperature ranges when both INP_D and INP_{MPOA} are included~~.~~ as independent INP sources. The ~~additional introduction~~addition of INP_{PBAP} ~~slightly reduces model skills for temperatures lower than −16°C~~does not enhance model's ability to reproduce the available observations; however, INP_{PBAP} ~~are the main contributors~~remains a key contributor to warm-temperature ice nucleation events. Therefore, consideration of dust ~~and,~~ marine and terrestrial ~~bioaerosol~~bioaerosols as distinct INP ~~precursors~~species is required to simulate ice nucleation in climate models. ~~In this respect, emissions, ice-nucleating activity of each particle type and its evolution during atmospheric transport require further investigations.~~

1 Introduction

Cloud ice exerts a multifaceted influence on climate (Zhang et al., 2020), affecting the radiative balance (Zhou et al., 2016; Yi, 2022), climate ~~feedback mechanisms~~feedbacks (e.g., temperature, albedo, water vapor feedbacks) (Choi et al., 2014), precipitation ~~patterns~~ (Sorooshian et al., 2009), and climate sensitivity (Murray et al., 2021). In mixed-phase clouds~~,~~ (MPC), ice particles and cloud droplets coexist in an unstable thermodynamic equilibrium owing to subzero temperatures. A significant feature of MPC is the degree of homogeneity of mixing ice particles and liquid droplets that affects the rate of precipitation formation (Korolev and Milbrandt, 2022). These clouds are prevalent throughout the troposphere, observed across all latitudes, spanning from polar regions to the tropics (D'Alessandro et al., 2019). ~~As a result, they significantly impact precipitation rates and the radiative energy balance on both regional and global scales.~~As a result, they significantly impact precipitation rates and the radiative energy balance on both regional and global scales (Hofer et al., 2024).

~~Within MPC, the interaction between ice particles and liquid droplets occurs through the molecular diffusion of water vapor. Ice particles~~In MPC, the most important ice formation process is immersion freezing, where an ice-nucleating particle (INP) becomes immersed in a supercooled droplet and initiates freezing, typically occurring between -5°C and -35°C (Pruppacher et al., 1998; Kanji et al., 2017 and references therein). Contact freezing happens when an INP collides with a supercooled droplet, triggering freezing on contact, often in turbulent conditions. This process is defined as separate from immersion freezing because of empirical evidence that some INP are more effective in this mode than when immersed in liquid (Shaw et al., 2005). Condensation freezing occurs when water vapor condenses and freezes simultaneously upon contact with an INP under specific supersaturation conditions. This process is less frequent compared to immersion freezing in atmospheric clouds (Vali et al., 2015). Deposition nucleation, where water vapor directly deposits as ice onto an INP without passing through the liquid phase, is more relevant at much colder temperatures (below -20°C) and is less significant in the typical temperature range of mixed-phase clouds (Kanji et al., 2017 and references therein) but it might still be important for cirrus clouds (Cziczo et al., 2013). Once forms, ice particles in MPC can grow at the expense of evaporating cloud droplets when the ambient water vapor

pressure lies between the ~~saturation~~ water vapor pressure with respect to ice ($e_{s,i}$) and water ($e_{s,w}$). This ~~case,~~is known as the Wegener-Bergeron-Findeisen (WBF) process, which is caused by the difference in supersaturation between the liquid and ice phases (Pruppacher et al., 1998), with the latter being consistently lower. Other factors that alter saturation water vapor pressure ~~can be~~are the vertical velocity as a source ~~for~~of water vapor, and the integrated ice crystal surface area, which depletes supersaturation by consuming the available water vapor (Korolev, 2007). ~~For the WBF process to occur, ice formation is first required, following two formation pathways: via homogeneous freezing at temperatures lower than −38 °C (Liu et al., 2012) or heterogeneous freezing at~~For the WBF process to occur, initial ice formation is required, which can happen through heterogeneous freezing at relatively warmer temperatures (Murray et al., 2012), ~~with the latter being~~a process that is crucial for ice formation in MPC while it can also occur in cold clouds. The presence of aerosols is necessary for heterogenous freezing since they provide a surface for the ice to form on. These aerosols called ice nucleating particles (INP), a select subgroup of aerosol particles - approximately 1 in 10^5 particles in continental air ~~are activated at~~ can activate temperatures warmer than -30°C (DeMott et al., 2010) - that initiate ice formation heterogeneously (Vali et al., 2015). Once the first ice crystals are formed, triggered by INP, they can rapidly grow via the WBF process and multiply via secondary ice processes (Georgakaki et al., 2022; Korolev and Leisner, 2020), therefore, affecting ~~precipitation ranges,~~ cloud properties~~,~~ and albedo.

The simulation of ice crystal concentrations in climate models is therefore important for determining the properties of ~~MPCs~~MPC, and uncertainties in the INP levels can lead to discrepancies in the modelled top-of-atmosphere radiative flux, and estimates of climate sensitivity to greenhouse gases (Vergara-Temprado et al., 2018; Murray et al., 2021). With climate change, and considering temperature changes alone, liquid water may progressively replace ice in MPC of a given altitude, making them more reflective. However, the magnitude of this so-called cloud-phase feedback is highly uncertain (Frey and Kay, 2018), partly due to uncertainties in the present and future spatiotemporal distribution of INP ~~(Zhao et al., 2021; Hoose et al., 2010; Raman et al., 2023)~~(Zhao et al., 2021; Hoose et al., 2010; Raman et al., 2023) and the structure of layered cloud systems that would promote glaciation through the seeder-feeder mechanism, where ice crystals from an upper cloud (seeder) fall into a lower-lying liquid cloud (feeder) and grow there by riming or vapor deposition via the WBF process (Ramelli et al., 2021). The inability of models to represent the occurrence frequency and glaciation state of MPC is also hypothesized as a major reason ~~making~~for disagreement between climate ~~models~~model results (Bodas-Salcedo et al., 2016) and reanalysis products (Naud et al., 2014) ~~disagree~~ with ~~each other in~~regard to the annual mean downward solar (short-wave, SW) radiation.

INP can originate from ~~a number of~~several sources, each with its own set of characteristics and properties. In the absence of ~~–~~a well-established theory for heterogeneous ice nucleation at temperatures warmer than -35°C, INP prediction typically relies on empirical parameterizations that are subject to considerable uncertainty and challenges. Advancing the predictability of INP abundance with reasonable spatiotemporal resolution will require an increased focus on research that bridges the measurement and modeling

communities. Additionally, coupling cloud processes to simulated ~~aerosol~~aerosols also makes cloud physics simulations increasingly susceptible to uncertainties in the simulation of INP, due to the lack of sufficient observational constraints.

Many substances have been shown to nucleate ice, depending on the cloud type and the predominant freezing mechanisms. ~~Reviewing experimental and modeling studies,~~However, observational evidence suggests that only a small number of particle types (<10) must be represented to adequately predict INP in climate models (Burrows et al~~. (~~., 2022) summarized the level of understanding and parameterisations of INP activity of 10 particle types that could represent INP in climate models.~~. In immersion freezing, which is the dominant mode of primary ice formation in MPC (Hande and Hoose, 2017), desert dust, marine primary organic aerosols (MPOA) and terrestrial primary biological aerosol particles (PBAP) have emerged as the most relevant INP ~~source~~types ~~(McCluskey et al., 2018; Chatziparaschos et al., 2023; Spracklen and Heald, 2014; Cornwell et al., 2023)~~(Spracklen and Heald, 2014; McCluskey et al., 2018; Chatziparaschos et al., 2023; Cornwell et al., 2023). These findings align with the physical understanding that INP are often efficiently activated as cloud condensation nuclei due to internal mixing with soluble components and their large size. These particles are likely enclosed within cloud droplets, making them available for immersion freezing but unavailable for contact freezing. The latter is constrained by the collision rate between interstitial particles and supercooled liquid droplets, a process that remains poorly understood at a fundamental level in real clouds (Kanji et al., 2017). Consequently, the role of contact freezing and its contribution to primary ice formation in MPC is characterized by high uncertainty.

1.1 Dust INP (INP_D)

Globally, airborne mineral dust from deserts and other drylands is considered the dominant INP source at temperatures below -20ºC (Murray et al., 2012; Kanji et al., 2017). For instance, Pratt et al. (2009) identified that ~50% of the ice crystal residual particles sampled in clouds at high altitudes over Wyoming were mineral dust. Studies have subsequently demonstrated that dust mineralogy plays a pivotal role in influencing the ice-nucleating efficiencies of mineral dust (Atkinson et al., 2013; Boose et al., 2016, 2019; Cziczo et al., 2013; Hoose et al., 2008), with several studies finding potassium enriched (K-) feldspar to be the most INP active dust mineral (Atkinson et al., 2013; Augustin-Bauditz et al., 2014; Zolles et al., 2015; Peckhaus et al., 2016; Harrison et al., 2019; Holden et al., 2019). Additionally, quartz is a major component of airborne mineral dust (Glaccum and Prospero, 1980; Perlwitz et al., 2015a, b) and exhibits a strong INP activity (Atkinson et al., 2013; Zolles et al., 2015; Losey et al., 2018; Kumar et al., 2019b; Holden et al., 2019). Quartz particles have substantially lower INP efficiencies than K-feldspar particles (Harrison et al., 2019), but their much higher abundance in the atmosphere can lead to an important INP ~~contributor~~contribution (Chatziparaschos et al., 2023). ~~Nevertheless, there~~ There are also other minerals present in ~~the atmosphere~~dust, such as smectite (Kumar et al., 2023) and kaolinite (Wex et al., 2014), but their ~~contribution~~activity is rather low compared to ~~INP levels remains unknown~~K-feldspar and quartz. Some laboratory studies have found that organic-rich soil

dust from agricultural lands is more INP active than inorganic desert dust (Suski et al., 2018), although this fraction is typically not represented in climate models (Burrows et al. 2022).

1.2 PBAP INP (INP_{PBAP})

While it is well established that dust particles are the most abundant source of INP at temperatures below -20ºC, it is equally well established that bioaerosols, i.e. atmospheric particles of biological origin, for instance terrestrial bioaerosol or PBAP, such as fungal spores, bacteria, pollen, and plant debris, are highly efficient ice nucleators at warm temperatures (Huang et al., 2021; Cornwell et al., 2022) and may have a substantial effect on ice crystal formation (Prenni et al., 2009). Only a small fraction of biological material can trigger ice nucleation (Huang et al., 2021), with INP concentrations estimated at approximately 1 to 2 per liter (Pöschl et al., 2010). These values are, however, about 2 orders of magnitude lower than the highest observed INP number concentrations from dust (Murray et al., 2012). Although these INP levels are much lower than usually observed for warm MPC, ice crystal formation from PBAP can be subsequently enhanced by ice multiplication processes ("secondary ice") (Korolev and Leisner, 2020), which are most efficient at temperatures warmer than -15ºC (Georgakaki et al., 2022; Sullivan et al., 2018). Recent advances in remote sensing and model/sensor fusion have enabled ~~the presence~~detection of secondary ice processes in clouds, revealing that ~~this process holds~~they hold particular significance in temperatures ranging from -5°C to -20°C (Wieder et al., 2022; Billault-Roux et al., 2023). At the same time, the presence of secondary ice particles (SIP) may actually mitigate uncertainties in INP predictions, given that ice crystal formation can be a self-limiting process (e.g., Sullivan et al., 2018).

Global simulations including biological particles have estimated that PBAP contribute to droplet freezing rates of clouds in the ~~warm~~warmer parts of mid-latitude ~~clouds, with about~~atmosphere, accounting for 1×10^{-5} % of the global average ice nucleation rates, ~~and~~with an upper-most estimate of 0.6% ~~(Hoose et al., 2010)~~(Hoose et al., 2010). ~~Spracklen and Heald, (2014) suggest that PBAP can dominate immersion freezing rates at altitudes between 400 and 600 hPa, in agreement with observational studies (Pratt et al.,~~Spracklen and Heald (2014) suggest that PBAP can dominate immersion freezing rates at altitudes corresponding to pressures between 400 and 600 hPa, in agreement with observational studies (Pratt et al., 2009). Field measurements have observed enhancements in both PBAP and INP related to rainfall events (Huffman et al., 2013; Tobo et al., 2013; Mason et al., 2015; Kluska et al., 2020) and suggested that PBAP emissions are affected by relative humidity (Prenni et al., 2013). Tobo et al. (2013) found that in a mid-latitude ponderosa pine forest, the variation pattern of INP concentration was like that of fluorescent biological aerosol particles during summertime, suggesting that PBAP ~~are~~is critical ~~contributors~~contributor to INP. Consequently, PBAP acting as INP at warm freezing temperatures may be an important ~~source~~type of INP in regions where they are abundant and may have a noteworthy impact on climate. However, modelling of PBAP remains challenging due to the complexity of ecosystem processes and a lack of observations (Burrows et al., 2022).

1.3 MPOA INP (INP_{MPOA})

Organic material with INP potential is also associated with sea ~~spay~~spray aerosol (SS) emissions from the ocean. Historically, SS was considered unimportant as a source of atmospheric INP. However, recent observational and modelling studies have revealed that emitted ~~MPOA~~SS mixed with ~~SS~~MPOA is potentially an important or even the only ~~source~~type of INP of marine origin ~~(Wilson et al., 2015; Mitts et al., 2021).~~(Burrows et al., 2013; Wilson et al., 2015; De Mott et al., 2016). McCluskey et al. (2018a, 2018b, 2019) confirmed that SS was strongly associated with MPOA as the primary organic INP source. Wilson et al. (2015) showed experimentally that marine organic material associated with phytoplankton and cell exudates in the sea surface microlayer is an important ~~source of~~contributor to atmospheric INP. In an exploratory model study, Burrows et al. (2013) showed that marine biogenic INP are likely to significantly contribute to the concentration of INP in the near-surface air over the Southern Ocean. INP derived from MPOA ~~have~~has potentially a remarkable effect on solar radiation, cloud glaciation and precipitation at high and mid-latitudes in remote marine regions especially during winter (Wilson et al., 2015). Huang et al. (2018) found that marine INP had only a small effect on cloud ice number concentration and effective radius, and did not significantly affect the global radiative balance. However, they emphasized that the relative importance of MPOA as an INP was found to be significantly dependent on the type of ice nucleation ~~parameterisation~~parameterization scheme that is chosen. Marine INP ~~are~~is not the main source of INP across all ocean areas. Gong et al. (2019) concluded that SS contributed less to the total INP in the atmosphere in Cape Verde than the other ~~precursors~~types of INP such as dust. In contrast, Vergara-Temprado et al. (2018) and McCluskey et al. (2019) proposed that MPOA ~~are~~is an important ~~source of~~contributor to INP in remote marine environments. ~~The largest~~Marine INP concentrations ~~of marine INP occur~~are found to maximize over areas of high biological activity and wind speed in the Southern Oceans, the North Atlantic, and the North Pacific~~ in regions where biological activity in surface ocean waters and wind speeds are greatest~~, while mineral dust from deserts (the ~~major~~main terrestrial ~~INP~~ source~~) only~~ of INP) accounts for only a small fraction of the INP observed ~~INP~~ in this region (Wilson et al., 2015; Huang et al., 2018).

In this study, we enhance our comprehension of the global spatiotemporal distribution of INP by incorporating both marine and terrestrial biogenic INP ~~precursors~~types, namely MPOA and PBAP, ~~here encompassing~~the latter including bacteria and fungal spores unless otherwise noted, building upon our earlier investigation of mineral dust-derived INP (Chatziparaschos et al., 2023). The methodology involves utilizing a 3-dimensional chemistry transport model for conducting simulations. Heterogeneous nucleation in the immersion mode is parameterized based on the singular hypothesis (Vali et al., 2015), using aerosol-specific parameters derived from laboratory and field observations. ~~Figure 1 presents a comprehensive schematic illustration of INP formation derived from mineral dust, MPOA and PBAP.~~ We identify major sources of INP and the specific aerosol types capable of acting as INP, dependent on location and season. ~~Additionally, we assess the relative contribution of bioaerosols to ice nucleation via immersion freezing in comparison to mineral dust and pinpoint regions and altitudes where this contribution holds significance. Simulated~~Figure

1 presents a comprehensive schematic illustration of INP derived from mineral dust, MPOA and PBAP that is used as the basis of our modelling approach. It includes emission processes, ice nucleation mechanisms, and the aerosol indirect effect, indicating the role of aerosols in cloud interactions and their impact on climate.

[FIGURE 1]

The simulations of INP-relevant species are evaluated with focus on the PBAP that is the new component in the model and its simulations have not been evaluated in earlier publications. Thus, the PBAP emissions, their seasonal variation, burdens and the calculated contributions are extensively evaluated against observations and other modelling studies. Furthermore, the simulated INP concentrations are rigorously evaluated against available INP observations sourced from the BACCHUS ~~(Impact of Biogenic versus Anthropogenic emissions on Clouds and Climate: towards a Holistic Under Standing; http://www.bacchus-env.eu/) and Wex et al. (2019) databases.~~and Wex et al. (2019) databases. For this purpose, INP concentrations are presented in this study in two ways as $[INP]_{ambient}$ and as $[INP]_{T;}$ $[INP]_{ambient}$ is calculated at ambient model temperature relevant to non-deep convective mixed-phase clouds using the ambient (model) temperature at each simulated level. $[INP]_{T}$ is calculated at a fixed temperature relevant to vertically extended clouds as deep-convective systems (Figure 1). $[INP]_{ambient}$ and $[INP]_{T}$ metrics can vary significantly. Finally, we assess the relative contribution of bioaerosols to ice nucleation via immersion freezing in comparison to mineral dust and pinpoint regions and altitudes where this contribution holds significance.

2. **Methods**

2.1 Model description

The well-documented 3-dimensional global chemistry-transport model TM4-ECPL (Kanakidou et al., 2020; Myriokefalitakis et al., 2015, 2016) is used here, driven by ERA-Interim reanalysis (Dee et al., 2011) meteorological fields from the European Centre for Medium-Range Weather Forecasts (ECMWF). The model is run with a horizontal resolution of 3° longitude by 2° latitude with 25 hybrid pressure vertical levels from the surface up to 0.1hPa (~ 65 km) and a model time step of 30 min. Therefore, we perform multi-year simulations that provide climatologically meaningful results. The TM4-ECPL model considers lognormal aerosol distributions in fine and coarse modes and allows hygroscopic growth of particles, as well as removal by large-scale and convective precipitation and gravitational settling. Advection of the tracers in the model is parameterized using the slopes scheme (Russell and Lerner, 1981), and convective transport is parameterized based on Tiedtke (1989) and the Olivié et al. (2004) scheme. Vertical diffusion is parameterized as described in Louis (1979). For wet deposition, both large-scale and convective precipitation are considered. In-cloud and below-cloud scavenging are parameterized in TM4-ECPL, applied as described by Jeuken et al. (2001) and references therein. For all fine aerosol components, dry deposition is

parameterized similarly to that of non-sea-salt sulfate, which follows Tsigaridis et al. (2006). Also, gravitational settling (Seinfeld and Pandis, 1998) is applied to all aerosol components.

2.2 Atmospheric cycle of INP-relevant aerosols

Desert dust emissions are calculated online as described in Tegen et al. (2002) and implemented as in ~~Van Noije et al. (2014).~~Van Noije et al. (2014) accounting for particle size distribution and based on vegetation type and cover, dust source areas, snow cover, soil moisture, and surface wind speed. Following Chatziparaschos et al. (2023), we consider both K-feldspar and quartz as the INP active mineral species of dust, whose fractions in the soil-surface are taken from the global soil mineralogy atlas of Claquin et al. (1999), with updates provided in Nickovic et al. (2012). The calculation of the emitted mass fractions of K-feldspar and quartz in the accumulation and coarse modes [with dry mass median radii (lognormal standard deviation) of 0.34µm (1.59) and 1.75µm (2.00), respectively] is based on brittle fragmentation theory (Kok, 2011). Thus, the mass emission of each mineral is calculated by applying the respective mineral-emitted mass fractions to the dust emission fluxes. All minerals are emitted externally mixed, and dust particle density is equal to 2650 kg m^{-3} (Ginoux et al., 2004; Tegen et al., 2002). ~~The modelled mineral dust mass concentration and deposition fluxes have been evaluated against global observations in a previous study (Chatziparaschos et al., 2023).~~

~~Terrestrial~~This study considers PBAP as terrestrial bacteria and fungal spores ~~are the PBAP considered in this study~~. In light of the well-documented discrepancies in INP activity spanning several orders of magnitude between various bioaerosol types (Murray et al., 2012; Kanji et al., 2017), it appears imprudent to assume that any individual species is representative of ambient PBAP. Therefore, we use parameterizations based on concurrent measurements of INP together with broad classification of bioaerosol (bacteria, fungal spore) types (Tobo et al., 2013). Terrestrial bacteria (BCT) emissions are parameterized as proposed in ~~Burrows et al. (2009b)~~Burrows et al. (2009), where near-surface observations were used in combination with model simulations to determine the optimal BCT flux rates for particles with a diameter of 1 µm [monodisperse spherical particles], across six different ecosystems: coastal: 900; crops: 704; grassland: 648; land ice: 7.7; shrubs: 502; and wetlands: ~~196m~~196 m^{-2} s^{-1}. For the present study, the Olson Global Ecosystem Database (Olson, 1992), originally available for 74 different land types on a spatial scale of 0.5◦×0.5◦, was grouped into 10 ecosystem groups as proposed by Burrows et al. (~~2009b~~2009). Consequently, the total bacteria flux is calculated as a sum of bacteria fluxes per ecosystem, weighted by the corresponding area of each ecosystem within the model's grid box. In TM4-ECPL, upon emission, the insoluble fraction of PBAP becomes progressively soluble due to atmospheric ageing. This process, which has been seen to occur, for instance, by degradation of RNA (Paytan et al., 2003) is parameterized based on the simulated oxidant levels, as for all other continental organic aerosols in the model (Tsigaridis and Kanakidou, 2003; Tsigaridis et al., 2006). Thus, the mean turnover of aged PBAP is estimated by applying a hydrophobic to hydrophilic conversion rate that depends on the atmospheric oxidants and is equivalent to a global mean turnover of 1.15 days

(Tsigaridis and Kanakidou, 2003; Kanakidou et al., 2012). Regarding deposition, the hydrophilic aerosols are removed from the troposphere faster by dry and wet deposition than the hydrophobic ones.

Fungal spores (FNG) fluxes are treated as linearly dependent on the leaf area index (LAI) and ~~the~~ specific humidity based on a parameterization proposed by Hummel et al. (2015). This parameterization is informed by field measurements of fluorescent biological aerosol particles conducted at diverse locations across Europe~~.~~; thus, it might not be very accurate for other regions and will be improved when data from other regions of the globe will become available. In the TM4-ECPL, the parameterization that is used to calculate FNG emissions online uses monthly averaged LAI distributions from the Global Land Cover 2000 database (European Commission, Joint Research Centre, 2003) as Hummel et al. (2015), which represents a climatology for the present study since no changes in vegetation from year-to year are taken into account, and 3-hourly averaged specific humidity and temperature data, as provided by ERA-Interim. Bioaerosol sizes range from fine to coarse, but since their shapes are not accurately known, for the present work, FNG are assumed to be monodisperse spherical particles of 3 μm diameter with 1000 kg m^{-3} density (Hummel et al., 2015). The organic matter to organic carbon ratio (OM:OC) of all PBAP is set equal to 2.6, and the molecular weight equal to 31 g mol^{-1}, using mannitol as a model compound (Heald and Spracklen, 2009; Myriokefalitakis et al., 2016).

The role of pollen as INP has been demonstrated in previous studies ~~(Hoose et al., 2010; Pummer et al., 2012)~~(Hoose et al., 2010; Pummer et al., 2012); however, its experimental determination is challenging due to its large size and spatiotemporal variability. With a mean diameter ranging from 10 to 125 μm (Jacobson and Streets, 2009) models assume that pollen is emitted as an entirely soluble aerosol (Hoose et al., 2010), resulting in substantial wet and dry deposition (Myriokefalitakis et al., 2017). Therefore, considering its size, pollen is anticipated to have much lower number concentrations compared to other PBAP at MPC altitudes, except possibly during periods of strong pollen emissions in the spring. However, pollen potentially impacts ~~at~~ low clouds as effective cloud condensation nuclei (Subba et al., 2023). Consequently, uncertainties in pollen emission, size distribution, hygroscopicity, and ice activity that ~~varies~~vary among pollen species (Pummer et al., 2015), lead us not to consider pollen as INP in this study. Overall, a fundamental understanding of bioaerosol types and the mechanisms of their emission from the biosphere into the atmosphere is lacking, highlighting the need for process studies to build confidence in INP model extrapolations in a changing biosphere.

MPOA emissions are calculated online by the model considering the partitioning between insoluble marine organics and sea salt, as described in detail in Myriokefalitakis et al. (2010). The parameterization is based on O'Dowd et al. (2008), modified by Vignati et al. (2010). MPOA is calculated as a fraction of the submicron sea-salt aerosol based on chlorophyll-a (Chl-a) present in the ocean surface layer. The organic mass fraction is calculated as a linear relation to Chl-a, valid for Chl-a concentrations below 1.43 μg m^{-3} (for larger values, the percentage is kept constant at 0.76). ~~Following sea-salt emission, MPOA is emitted, assuming that it is~~

~~entirely insoluble, as determined by O'Dowd et al. (2008). The final MPOA diameter is dependent on Chl-a uptake (Vignati et al., 2010), scaling to a minimum diameter of 0.09 μm.~~MPOA is emitted in the fine mode together with SS with a magnitude that depends on Chl-a in the seawater and assuming that it is entirely insoluble as determined by O'Dowd et al. (2008) and applying the same modeling approach as in Vignati et al. (2010). Additionally, based on Facchini et al. (2008), we adopted a coarse mode MPOA source (Gong, 2003; Myriokefalitakis et al., 2010). The sea-salt source is calculated online by TM4-ECPL driven by wind speed at every time-step, following Gong (2003) and fitted for accumulation and coarse modes as described in Vignati et al. (2010). In TM4-ECPL, Chl-a concentrations are satellite-derived monthly average MODIS observations at a resolution of 1°x1°. The density of water-insoluble organic mass was set to 1000 kg m^{-3} (Vignati et al., 2010) and that of dry sea salt to 2165 kg m^{-3} (O'Dowd et al., 2008). The ageing of insoluble MPOA is taken into account, ~~as for all other insoluble primary organic aerosols in the model, and~~applying a constant first order loss rate that corresponds to a global mean turnover time of about 1 ~~day~~.15 days (Cooke et al., 1999; Tsigaridis and Kanakidou, 2007). ~~Model results have been evaluated against observations in the marine environment by comparing water insoluble organic carbon observations with modelled insoluble MPOA, as referred in Myriokefalitakis et al. (2010).~~

2.3 Ice nucleation parameterizations

2.3.1. ~~*Desert*~~Mineral dust: K-feldspar and quartz

The effect of dust minerals on the INP concentration is parameterized using the singular approximation based on the laboratory-derived active site density parameterizations for K-feldspar and quartz minerals provided in Harrison et al. (2019). The parameterization for K-feldspar is valid in the temperature range between -3.5°C and -37.5°C, while for quartz, between -10.5°C and -37.5°C. To calculate aerosol surface area, we assume that each mineral dust particle is spherical and externally mixed (Atkinson et al., 2013; Vergara-Temprado et al., 2017). The density of ice nucleation active surface sites, derived from ~~the spectrum of~~ ice nucleation ~~properties and~~frozen fraction for a polydisperse aerosol sample, is assumed to follow a Poisson distribution:

$$\sim\sim INP_D = \sum_i \sum_j n_{i,j} \left\{1 - e^{[-S_{i,j} n_{s(i)}(T)]}\right\} \text{INP}_D \sim\sim = \sum_i \sum_j \text{n}_{i,j} \left\{1 - \text{e}^{[-\text{S}_{i,j} \text{n}_{s(i)}(T)]}\right\} \quad \text{Eq. } 1\sim\sim 1$$

where INP_D is the number concentration of ice formed on the mineral dust aerosol, ~~$n_{i,j}$~~$\text{n}_{i,j}$is the total dust mineral particle number concentration (per m^{-3}), where index ~~i~~i corresponds to mineral type (quartz and K-

feldspar) and index ~~*i*~~j to size mode (accumulation and coarse mode). ~~$S_{i,j}$~~$S_{i,j}$ is the individual dust particle mean surface area (cm^{-2}) in size mode ~~*i*~~j. Air temperature, ~~*T*~~T, is given in degrees Kelvin and ~~$n_{s(i)}$~~$n_{s(i)}$ corresponds to the active site density of each mineral (Harrison et al., 2019). Further details on the methodology and the evaluation of the simulated INP derived from mineral dust are provided in Chatziparaschos et al. (2023).

2.3.2 PBAP~~:~~

The number concentration of INP derived from PBAP is based on the parameterization of Tobo et al. (2013), which considers the dependence of INP on temperature and the number concentration of aerosol particles with diameters larger than 0.5μm. Particles with diameters above this threshold are assumed to have a sufficient surface area to provide active sites for ice nucleation (DeMott et al., 2010). Tobo et al. (2013) derived a parameterization of INP_{PBAP} from observations of INP and ambient fluorescent biological aerosol particles (FBAP) in a mid-latitude ponderosa pine forest ecosystem. They, thus, proposed to calculate INP_{PBAP} number concentration for temperatures ranging from about -9°C to -34°C and the number ~~concentrations~~concentration of FBAP, hereafter replaced by that of PBAP, as follows:

~~INP_{PBAPs}~~

~~$= \left(N_{PBAPs,>0.5\mu m}\right)^{\alpha'(273.16-T)+\beta'} e^{\gamma'(273.16-T)+\delta'}$~~ $\mathrm{INP_{PBAP}}$

$= \left(\mathrm{N_{PBAP,>0.5\mu m}}\right)^{\mathrm{a'(273.16-T)+\beta'}} \mathrm{e^{\gamma'(273.16-T)+\delta'}}$ Eq. ~~2~~2

where $\alpha' = -0.108$, $\beta' = 3.8$, $\gamma' = 0$, and $\delta' = 4.605$ and N_{PBAP} is the number concentration (m^{-3}) of PBAP (FNG and BCT) larger than 0.5μm, and T is the air temperature in Kelvin. There are two limitations in using this parameterization. Firstly, this parameterization has been derived from a mid-latitude ponderosa pine forest ecosystem and therefore its application on a global scale remains a rough approximation. Secondly, FBAP may also contain non-PBAP (e.g., mineral dust particles, secondary organic aerosol particles) that contribute to fluorescence (Bones et al., 2010; Lee et al., 2013; Morrison et al., 2020). The number fractions of FBAP to the total aerosol particles in the super-micron size range could be relatively similar to those of PBAP under dry conditions (Tobo et al., 2013). Indeed, observations by Negron et al. (2020) suggest that airborne bacteria may be unambiguously detected with autofluorescence. ~~However, during and after rain events, PBAP were underestimated~~ However, during and after rain events, PBAP were underestimated by more than a factor of 2 (Huffman et al., 2013), suggesting that FBAP reflect only a portion of PBAP. ~~Additionally, observations by Negron et al. (2020) suggest that airborne bacteria may be unambiguously detected with autofluorescence.~~ Overall, there is ample evidence supporting a correlation between INP and total fluorescent particles (Huffman et al., 2013). However, the exact identity of these fluorescing particles has not yet been clarified adequately, and it remains challenging to determine better proxies for biological origin INP that can be readily measured in the environment.

2.3.3 MPOA

The contribution of marine organic material to INP is parameterized according to Wilson et al. (2015), based on the total organic carbon (TOC) in the sea spray originating from the sea surface microlayer and the ice-nucleating temperature. It considers the active sites density per unit mass of TOC contained in insoluble MPOA and is derived from a spectrum of temperatures ranging from -6°C to -27°C. A factor of 1.9 is used for the conversion between MPOA and TOC in the model, as suggested in Burrows et al. (2013). The number concentration of INP_{MPOA} (m^{-3}) per TOC (g) originating from MPOA is calculated following the equation below.

$$INP_{MPOA} = C_{MPOA} e^{[11.2186-(0.4459*T)]} \mathrm{INP}_{\mathrm{MPOA}} = \mathrm{C}_{\mathrm{TOC}} \mathrm{e}^{[11.2186-(0.4459*\mathrm{T})]} \quad \text{Eq. 33}$$

where C_{TOC} $\mathrm{C}_{\mathrm{TOC}}$ is the total organic carbon mass concentration (g/m^3) of marine particles and T T is the air temperature in °C.

2.4 Simulations and INP evaluation

Simulations were performed from 2009 to 2016 using the year specific meteorological fields and emissions as described in the previous sections. Prior to the evaluation of INP, we provide an evaluation of the INP-relevant aerosols. The simulated mineral dust mass concentrations and deposition fluxes were evaluated against global observations in Chatziparaschos et al. (2023), and a summary of the evaluation is presented below. We also assess the MPOA simulations using observations from Mace Head and Amsterdam Island, incorporating findings from multiple studies (Sciare et al., 2009; Rinaldi et al., 2010). Evaluations of PBAP, as well as individual BCT and FNG concentrations, are based on a compilation of long-term measurements of atmospheric fluorescent bioaerosols and number concentrations from various locations, as listed in Elbert et al. (2007), Bauer et al. (2008), Burrows et al. (2009) and Genitsaris et al. (2017).

The simulated INP are compared against the available INP observations from the databases of BACCHUS (Impact of Biogenic versus Anthropogenic emissions on Clouds and Climate: towards a Holistic Under Standing) (http://www.bacchus-env.eu/in/index.php, last accessed on 26 March 2020) and Wex et al. (2019) (https://doi.pangaea.de/10.1594/PANGAEA.899701, last access on 14 February 2022). The observational data span from 2009 to 2016 and originate from different campaigns (locations are shown in supplementary Fig. S1). For this comparison, INP concentrationsAs outlined in the introduction $[INP]_T$ and $[INP]_{ambient}$ are determined by the simulated particle concentration and for $[INP]_T$ a specific temperature (T), while for $[INP]_{ambient}$ the model's ambient temperature is used. $[INP]_T$ is the appropriate metric when comparing modelled INP concentrations to observations, as measurements are typically conducted by exposing particles to specific, controlled temperatures within the instruments. Thus, for the model evaluation, $[INP]_T$ concentrations are used that are calculated at the temperature at which the measurements were performed. All model results are compared to observations for the specific month and year as well as the location of

observation, except for those reported by Yin et al. (2012) and Bigg campaigns (Bigg, 1990, 1973), which cover temporally scattered measurements (between 1963 and 2003) and are therefore compared to the modelled multi-annual monthly mean INP concentration from 2009 to 2016. Two statistical metrics are used to assess the ability of the model to correctly predict INP concentrations: i) the percentage of INP simulated values within one order of magnitude from the observed values (Pt_1) and ii) the percentage within one and half orders of magnitude ($Pt_{1.5}$). The correlation between observed and predicted INP (as log/log regression) is presented by the correlation coefficient (R) of the regression of the logarithms of the concentrations.

~~3~~

3. Results and Discussion

3.1 INP-relevant aerosols

3.1~~.~~1 Global ~~INP distributions~~simulations

Figure 2 ~~depicts~~displays the annual ~~zonal~~ mean ~~profiles of INP number~~surface concentrations ~~that are derived from mineral dust, PBAP~~of dust (K-feldspar and quartz), marine primary organic aerosol (MPOA ~~(INP_D, INP_{PBAP},)~~, and ~~$INP_{MPOA,}$ respectively) (Fig. 2a-c)~~primary biological aerosol particles (PBAP), with PBAP components shown separately as bacteria (BCT) and fungi (FNG), along with their zonal mean distributions as calculated by the model, averaged over the study period. A portion of these aerosols act as INP, as discussed in Section 2.3. Dust aerosols peak over desert regions and exhibit notable concentrations in the outflow regions of the Sahara and Gobi deserts, predominantly in the Northern Hemisphere (NH), as well as downwind of Patagonia over the South Atlantic. MPOA, driven by surface wind speeds and seawater chlorophyll levels, reaches its highest concentrations in the high latitudes of both the NH and Southern Hemisphere (SH). BCT and FNG concentrations peak over continental regions, particularly across tropical zones.

[FIGURE 2]

3.1.2 Evaluation of simulated INP-relevant aerosols

3.1.2.1 Dust

The modelled mineral dust mass concentration and deposition fluxes were thoroughly evaluated against global observations in a previous study (Chatziparaschos et al., 2023). A monthly-collocated evaluation of the modelled dust surface concentration was performed against in-situ measurements representative of Saharan dust sources and transport regions from four stations (M'Bour, Bambey, Cinzana, and Banizoumbou) located at the edge of the Sahel (Lebel et al., 2010), three stations (Miami, Barbados, and Cayenne) located on the American continent, downwind of the Atlantic dust transport (Prospero et al., 2020), and two stations, Finokalia (Crete, Greece) (Kalivitis et al., 2007) and Agia Marina (Cyprus) (Pikridas et al.,

2018) situated along the dust transport over Mediterranean. This comparison suggested a slight positive bias (modelled concentrations were compared with, located in regions well suited for studying results 8.3 µg m^{-3}on average, i.e. representing 5 %) average dust. The ability of TM4-EPCL to represent the global dust cycle was further evaluated against the modelled surface dust concentration and deposition with climatological, globally distributed observations [Climatological annual means of dust surface from the Rosenstiel School of Marine and Atmospheric Science (RSMAS) of the University of Miami (Arimoto et al., 1995; Prospero, 1999) and the African Aerosol Multidisciplinary Analysis (AMMA) (Marticorena et al., 2010)]. A tendency to overestimate dust surface concentrations was also noted in comparisons with these annual mean climatological observations, with an overall normalized mean bias of 44.1%. For deposition model errors were higher than for surface concentration fields, with a normalized mean bias of 59.2 %. Despite these discrepancies, which must be considered in evaluating INP simulations, the model reliably captures the geographic distribution of atmospheric dust within an acceptable order of magnitude.

3.1.2.2 MPOA

The evaluation of organic carbon derived from MPOA was previously conducted by Myriokefalitakis et al. (2010), estimating an annual global source of MPOA about 4 $TgC \cdot yr^{-1}$. TM4-EPCL captures the general geographic variability, although it tends to underestimate organic carbon concentrations, suggesting a possible underestimation of emissions or missing sources. The uncertainties are particularly tied to parameterizations of sea spray emissions, which are highly variable spatially and temporally and are estimated to affect the MPOA concentrations by a factor of 4, as well as to the fractional contribution ~~to the total INP concentration~~ of organic matter in sea spray particles that has on average an uncertainty of 33% (Vignati et al., 2009). We further evaluate the MPOA concentrations and MPOA fraction in SS by comparison with observations from Mace Head (North Atlantic; Rinaldi et al. (2010)) and Amsterdam Island (Austral Ocean; Sciare et al. (2009)) as depicted in Figure 3.

[FIGURE 3]

Figure 3a compares simulated MPOA concentrations (averaged over the simulation period) with marine sector observations at Mace Head in 2006 (Rinaldi et al., 2010; total water-insoluble and water-soluble organic matter). The model generally captures the seasonal pattern, with elevated values in spring and summer and lower values in winter, but tends to slightly underestimate the annual mean concentration by about 3%. The underestimation is most pronounced in summer, while spring and fall values appear to be overestimated. Observed organic carbon (OC) levels at Amsterdam Island in the Austral Ocean, measured from 2003 to 2007 by Sciare et al. (2009), are primarily attributed to MPOA (Myriokefalitakis et al., 2010) and are compared with model results in Figure 3b. Overall, the model underestimates the observations by 50% with the largest discrepancy in Austral summer. When comparing observations from both the Northern and Southern Hemispheres to model results (Figure S2) an overall underprediction of 29% (nMB) is evident. These

discrepancies may reflect deficiencies in the applied MPOA source and sink parameterizations. Sea salt emissions and chlorophyll-a concentrations, are key drivers of the spatial distribution of MPOA, and play a significant role in this discrepancy. Furthermore, the coarse resolution of the model may not capture sharp latitudinal gradients in localbiological activity. A possible underestimation of the marine source associated with the specific distribution of phytoplankton species, in addition to the use of monthly averages for Chl-a from MODIS, which can smooth out short-term variations, can significantly affect MPOA emissions. Therefore, a factor of two uncertainty in the simulated MPOA is plausible and the observed underprediction (3%-50%) should be considered when evaluating the INP simulations.

3.1.2.3 PBAP

The simulated BCT, FNG, and total PBAP number concentrations are compared with observations at various locations in Figures 4a-c. Figure 4a presents the comparison of simulated BCT with observations from Burrows et al. (2009) and Genitsaris et al. (2017). Actively wet discharged ascospores (AAS) and basidiospores (ABS) data are compared with simulated FNG (Figure 4b). AAS and ABS are assumed to contribute one-third each to total fungal spore concentration (Burrows et al., 2009). The observations are listed in Elbert et al. (2007) [AAS-ABS] and Bauer et al. (2008) [fungal spore concentrations].

[FIGURE 4]

Figure 4a shows that the model underestimates BCT concentrations across most regions and seasons by 75% (nMB) on average. This bias may be partly due to the monodisperse approach of bacterial emissions or their assumed diameter (1μm). The comparison of ABS and AAS with simulated FNG (Figure 4b) following the approach of Hoose et al. (2010) shows both significant overestimation and underestimation by the model, but the FNG concentrations listed in Bauer et al. (2008) agree well with the simulated concentrations, which assume a monodisperse aerosol of 3 μm diameter. Overall, simulations of fungal spores tend to overestimate measurements with a nMB of 7.2%. Taking into account that the model results are monthly averages for the 2°×3° model grids and thus their comparability with point measurements is limited, as well as the uncertainties in the observations and their spatial and temporal representativeness, the agreement between measurements and observations is satisfactory overall.

Although the simulated BCT concentrations are underestimated, the total PBAP (BCT, FNG and pollen) number concentrations are in the correct order of magnitude when compared to fluorescent PBAP number observations averaged over the reported period (Figure 4c); the model tends to overestimate total PBAP by 17%. Furthermore, the model captures reasonably well the seasonal variations that follow the observed patterns (Supplementary Figure S3), although it tends to overestimate the total PBAP number concentration, in summer and autumn, when biological activity is high. This may indicate that either fungal spores or pollen may be less important contributors to the total PBAP number at the monitoring sites than simulated. The

discrepancy between model simulations and observations highlights the complexity of biological aerosol emissions and the influence of local environmental factors on bioaerosol concentrations.

In summary, the evaluation of INP-relevant aerosols simulations shows that the model underpredicts MPOA (by about 30%; 3% - 50%) and overpredicts dust surface concentrations and deposition (by about 60%). PBAP concentrations are also slightly overpredicted (by about 20%), with BCT being significantly underpredicted and FNG moderately overpredicted. The model captures the seasonal variation of observed PBAP, while the simulated MPOA in the SH shows no significant variation across seasons. These model features must be taken into consideration when discussing the results of the INP simulations, since uncertainties in the INP simulations include uncertainties in both the INP parametrization and INP-relevant aerosol simulated concentrations and are affecting the importance of various INP types.

3.2 Global INP simulations

3.2.1 INP global distributions

Figure 5 (a-c) depicts the simulated spatial distributions of INP concentrations derived from each studied aerosol type present at 600 hPa and with the ability to freeze at -20°C in immersion mode (hereafter called INP_D at -20°C and noted as INP_D[600hPa, -20ºC], INP_{MPOA} at -20°C and noted as INP_{MPOA}[600hPa, -20ºC] and INP_{PBAP} at -20°C and noted as INP_{PBAP}[600hPa, -20ºC], that is INP from dust, MPOA and PBAP (BCT and FNG), respectively). (This metric is explained in Sect. 2.4 and Figure 1 $[INP]_T$.) The chosen pressure level is representative of the low free troposphere and average temperatures broadly consistent with those of the INP measurements. These conditions of temperature and pressure are representative of MPC's glaciation. Figure 5d shows the total $[INP]_T$ distribution calculated accounting for all the INP types.

[FIGURE 5]

INP_D[600hPa, -20ºC] (Fig. 5a) are higher in the mid-latitudes of the NH than in the SH due to the location of dust sources and long-range atmospheric transport patterns that favor the presence of atmospheric dust in the NH. Throughout much of the low and mid-latitudes of the NH, INP_D[600hPa, -20ºC] outnumbers by far INP_{MPOA}[600hPa, -20ºC] and INP_{PBAP}[600hPa, -20ºC] (Fig. 5a-c). ~~2d-f). INP$_D$~~INP_{MPOA} at -20ºC dominates in the oceanic regions, particularly in the SH, and INP_{PBAP}[600hPa, -20ºC] prevails over tropical and equatorial continental sites and up to +/- 40º latitude.

Remarkably, there are oceanic regions in the South Atlantic Ocean and Pacific Ocean (such as the south hemisphere tropical west coasts of South Africa and South America) where PBAP has the potential to form ice crystals at the outflow of the continental air (Fig. ~~2a) present~~5d, circles 1 and 5), enhancing INP concentrations in marine atmosphere. These findings indicate that PBAP derived from terrestrial vegetation

ecosystems can play a significant role in driving atmospheric INP concentrations both within and downwind of source areas.

In addition to the presence and thus potential influence of PBAP in marine environments, INP_D[600hPa, -20°C] shows considerable levels in many oceanic regions. This is particularly evident over the central Atlantic, downstream of the Sahara, where INP_D[600hPa, -20°C] surpass those of both INP_{MPOA}[600hPa, -20°C] and INP_{PBAP}[600hPa, -20°C] (Fig. 5d, circle 2). INP_D[600hPa, -20°C] shows also significant levels over the North Pacific, where dust is carried by continental outflows. Mineral dust and MPOA control the INP population over the South Atlantic adjacent to northeastern coast of South America due to both emissions from the Patagonia desert and marine biota (Fig. 5d, circle 3). Over the southern Indian Ocean INP_{MPOA}[600hPa, -20°C] dominates (Fig. 5d, circle 4). The simulated increase of INP by MPOA towards the SH isis consistent with findings by Huang et al. (2018). Figure 6 depicts multi-annual zonal mean vertical profiles of ambient INP number concentrations that are derived from mineral dust, PBAP and MPOA calculated at modelled ambient temperature (INP_D, INP_{PBAP}, and INP_{MPOA}, respectively; [$INP_{ambient}$] shown in Figure 1) (Fig. 6a-d) along with the total ambient INP concentration (Fig. 6d).

[FIGURE 6]

INP_D (Fig. 6a) presents considerable concentrations (>$5x10^{-1}$ L^{-1}) at temperatures ~~colder than~~below -20°C in agreement with findings by Hoose and Möhler (2012). Previous studies suggested that dust is the dominant source of immersion mode INP at temperatures colder than −25°C (Murray et al., 2012; Kanji et al., 2017). However, over the dust belt, dust has been found to initiate freezing in midlevel supercooled stratiform clouds at temperatures of −10°C and below (Liu et al., 2008; Zhang et al., 2012). These ~~are warmer~~ temperatures are warmer than those reported by Ansmann et al. (2008), who found no evidence of ice formation in supercooled stratiform clouds with cloud-top temperatures above −18°C, but colder temperatures than those found by Sassen et al. (2003), who attributed the glaciation of altocumulus clouds at −5°C to African dust. Although mineral dust can act as INP at warm temperatures, this depends on, among other factors, ~~the amount~~type and fraction of different minerals [K-feldspar and quartz fraction (Chatziparaschos et al., 2023; Harrison et al., 2019)], particle size (Chen et al., 2021), particle concentration per droplet, and biological nanoscale fragments attached to dust particles (Augustin-Bauditz et al., 2016). ~~Our model results show that PBAP are the primary source of INP between −12°C and −20°C.~~In our model, the potential mixing of dust with biological material is not considered and INP types are assumed to be externally mixed aerosols. ~~This agrees with a recent observational and modelling study by Cornwell et al. (2023). Overall, mineral dust (Fig. 2d) dominates INP levels at high altitudes almost over the globe in all seasons (Fig. S2). At intermediate pressure levels (up to 600hPa and T < -20 °C), INP_D dominate over the North Hemisphere (NH) (Chatziparaschos et al., 2023), where the major sources of dust minerals are located (Sahara, Gobi deserts and Arabian Peninsula). Between 20°S and 90°N, the simulated concentrations of INP are driven mostly by~~

~~mineral dust and PBAP. MPOA plays a minor role, contributing less than 30% between 800 to 600 hPa (60 to 90°N).~~

The simulated INP_{PBAP} shows high number concentrations with concentrations >10 L^{-1} at low altitudes between 40°S and 90°N at temperatures warmer than -16ºC (Figure 6c). The temperature range where simulated INP_{PBAP} exhibit considerable concentrations is close to the temperature range where secondary ice formation is expected to be active, i.e., between -5ºC and -20ºC (Korolev and Leisner, 2020), with peak impact around -15 ºC (Georgakaki et al., 2022). Therefore, although not contributing significant primary ice particles, INP_{PBAP} may help sustain secondary ice formation, by contributing primary ice at relatively warm freezing temperatures for SIP. That said, SIP is most effective for situations where there are seeder-feeder cloud configurations (i.e., layered clouds or vertically developed clouds that have internal seeding; Georgakaki and Nenes, 2023) so it remains to be investigated whether the "niche" impact of INP from PBAP on SIP is climatically important.

The simulated INP_{MPOA} number concentrations are low (10^{-1} to 1 L^{-1} at 800hPa, <-20ºC; Figure 6b) and consistent with the simulated concentration range shown in Wilson et al. (2015) and Vergara-Temprado et al. (2018). Despite the relatively large sources of MPOA in the SH, a region mostly covered by oceans, the resulting INP_{total} concentrations remain lower than those simulated over the NH (Figure 6d), which is mostly continental and where dust and PBAP are mainly present. This pattern of low INP concentration in the SH agrees with observations in the Southern Ocean (McCluskey et al., 2018; Welti et al., 2020). The relatively low INP_{MPOA} number concentrations in the SH (Figures 5b, 6b) could be translated into less cloud droplet freezing, enhancing cloud reflectivity (Vergara-Temprado et al., 2018). Low INP concentrations could lead to the initial growth of large ice (i.e., in the seed region) and can influence the evolution of the microphysical cloud structure in the lower cloud levels (i.e., in the feeder region) enhancing precipitation (Borys et al., 2003; Ramelli et al., 2021). Vergara-Temprado et al. (2018) suggest that INP_{MPOA} are negatively correlated with shortwave (SW) radiation up to an INP concentration of 1 L^{-1}, above which the reflected radiation drops sharply as the ice processes become more efficient and deplete most of the liquid water.

3.2.2 Contribution of INP types to the total INP

Figure 7 shows the multi-year average zonal mean of the percentage contribution of each INP type to the total INP as simulated by the model. INP_{PBAP} is the primary type of INP between −12°C and −20°C. This agrees with a recent observational and modelling study by Cornwell et al. (2023). Overall, mineral dust (Fig. ~~INP_{PBAP} are important at low altitudes between 40°S and 90°N with concentrations >10 L^{-1} at -16ºC. Their contribution to the total INP is more than 80% between -12ºC to 16ºC. PBAP are~~7d) dominates INP levels at high altitudes in most of the globe in all seasons (Fig. S3). At intermediate pressure levels (up to 600hPa and T <-20 ºC), INP_D dominates over the North Hemisphere (NH), where the major sources of dust minerals are located (Sahara, Gobi deserts and Arabian Peninsula), as also reported by Chatziparaschos et al. (2023). Between 50°S and 90°N, the simulated concentrations of INP are driven mostly by mineral dust and PBAP.

MPOA plays a minor role there, contributing less than 20% of the total INP between 800 and 600 hPa (60°N and 90°N).

[FIGURE 7]

PBAP is more ice-active than mineral dust at relatively high temperatures (Murray et al., 2012; Tobo et al., 2013; Harrison et al., 2019). ~~INP_{PBAP} mainly affect~~Therefore, INP_{PBAP} contribution to the total INP is more than 80% between -12ºC and -16ºC. INP_{PBAP} mainly affects the tropical and subtropical atmosphere during the whole year at temperatures higher than about -16ºC ~~over the SH and extend to pole in the NH. In boreal summer, due to vegetation growth, the INP_{PBAP} fractional contribution is shifted towards northern latitudes (Fig. 2S). Our results suggest that PBAP derived from forest biota play an important role in driving atmospheric INP concentrations both nearby and downwind of these ecosystems. They also show that PBAP may be the dominant precursor of INP at relatively warm temperatures, as has been previously suggested~~and extends to the pole in the NH. Note that MPC were found to occur more frequently in the convective towers in the tropics than at the mid-latitudes and the Arctic (Costa et al., 2017). In the boreal summer, the high INP_{PBAP} contributions to total INP are shifted to northern latitudes due to vegetation growth (Fig. S4). These results suggest that PBAP may be the dominant type of INP at relatively warm temperatures, consistent with previous studies (Tobo et al., 2013; Murray et al., 2012; DeMott and Prenni, 2010). At temperatures colder than -20°C, nonbiological aerosol particles ~~like~~such as mineral dust are effective INP (Murray et al., 2012; Si et al., 2019)~~, thus dominating~~ and dominate the INP population~~.~~ (Fig. 7a). In the NH, INP concentrations mainly originating from PBAP and mineral dust are higher than those in the SH where INP_{MPOA} dominates between 60°-90°S. The impact of INP_{MPOA} is notably more pronounced in the SH, due to the high levels of INP_{PBAP} and INP_D concentrations in the NH. There is a pronounced seasonality in dust INP (Figure S5), with large concentrations observed between 40°N and 90°N during the boreal winter and spring (DJF, MAM) when transported dust can influence INP concentration over the Arctic. In contrast, INP_{MPOA} shows minimal seasonal variation and consistently dominates the SH between 40°S and 80°S. Between 60°S and 60°N, INP_{PBAP} is the most prevalent INP type at higher pressure and temperature levels, especially in the NH during the boreal summer (JJA) and autumn (SON), when its contribution to total INP increases.

~~The simulated low INP_{MPOA} number concentrations (10^{-1} to $1L^{-1}$ at 800hPa, <-20ºC) are consistent with the concentration range shown in Wilson et al.~~ Thus, the seasonal variation of INP composition highlights the influence of temperature, atmospheric circulation, and biological activity on INP. At low altitudes and warm temperatures, INP populations are influenced by the prevalence of INP of biological origin (INP_{MPOA} and INP_{PBAP}), with MPOA affecting INP concentrations mainly in the SH and PBAP in the NH. INP_D is the primary contributor to the INP population at high altitudes, where temperatures are low, displaying a consistent pattern across all seasons.

Figure 8 provides a comprehensive view of the global distribution of INP in the tropospheric column from the surface up to 300 hPa (Fig. 8a), calculated at the ambient modelled temperature, as well as the percentage contribution of each INP type per season and for three latitudinal zones (Fig. 8c). High INP column burdens are simulated in the NH and especially over the Sahara, parts of the Middle East, and the northern part of South America. These regions are known to be significant dust emission and biological aerosol sources (Amazon). Lower INP column burdens are simulated over the polar and oceanic regions, indicating that the contributions from INP sources in these areas are limited. The simulated INP column burdens are~~(2015) and Vergara-Temprado et al. (2018). Despite the relatively large sources of MPOA in the SH, a region covered mostly by sea, the resulting INP_{total} concentrations remain lower than those simulated over the NH, mostly continental, where dust and PBAP dominate. This pattern of low INP concentration in the SH agrees with observations in the Southern Ocean (Chubb et al., 2013) and could be translated into less cloud droplet freezing, enhancing cloud reflectivity (Vergara-Temprado et al., 2018). However, low INP concentrations could lead to the initial growth of large ice (i.e., in the seed region) and can influence the evolution of the microphysical cloud structure in the lower cloud levels (i.e., in the feeder region) enhancing precipitation (Borys et al., 2003; Ramelli et al., 2021). Significant radiation biases in the models occur mainly in remote marine regions away from major INP sources, where the prevalence of MPOA results in uniquely low INP concentrations (Vergara-Temprado et al., 2018). On a global scale, the small number of INP contributed by MPOA and the low sensitivity of cloud ice properties to ice nucleation, as suggested by Huang et al. (2018), imply that MPOA do not significantly affect the radiative balance. However, the relative importance of MPOA as an INP in the models depends strongly on the type of ice nucleation parameterisation scheme chosen (Huang et al., 2018). For instance, Vergara-Temprado et al. (2018) propose that the low INP_{MPOA} concentrations are essential to cloud reflectivity. They suggest that INP_{MPOA} are negatively correlated with shortwave (SW) radiation up to an INP concentration of 1 L^{-1}, above which the reflected radiation drops sharply as the ice processes become more efficient and deplete most of the liquid water. According to Huang et al. (2018), MPOA lead to a considerable increase in INP concentrations close to the surface in the polar regions as also here calculated and shown in figure 2c. Nevertheless, the impact of INP_{MPOA} is notably more pronounced in the SH, due to the increased competitiveness of INP_{PBAP} and INP_D concentrations in the NH. All in all, at high pressure levels, INP populations are influenced by the prevalence of bio-INP (INP_{MPOA} and INP_{PBAP}), with MPOA affecting INP concentrations mainly in the SH and PBAP in the NH.

Similar patterns emerge from the zonal mean seasonal analysis (Fig. S2). In the boreal winter and spring months (DJF, MAM), INP_D dominates at low pressure levels between 60°-90°N, with INP_{MPOA} contributing less than 30%. Meanwhile, between 60°S-60°N, INP_{PBAP} are prevalent but with low concentrations. INP_D remains the primary contributor to INP population at high altitudes, displaying a consistent pattern across all seasons. In JJA and SON, INP_{PBAP} and INP_{MPOA} dominate at low altitudes, showing alternating patterns influenced by vegetation and ocean biota. The recent observational study by Creamean et al. (2022) in the central Arctic revealed a strong seasonality of INP during the year, with lower concentrations in the winter

and spring controlled by transport from lower latitudes, to enhanced concentrations of INP in the summer, likely from marine biological origin. This only partially agrees with our results showing that INP concentrations are influenced by transported airborne dust in winter, but INP_{PBAP} contribute more than INP_{MPOA} in summer. At warm temperatures (above -16 °C) in the Arctic, the majority of simulated INP are typically biological throughout the year. While at lower temperatures, INP are from continental sources (e.g. dust) and are mostly inorganic (INP_D).

Our findings highlight that INP at warm temperatures primarily derive from organic sources, as simulated by PBAP and MPOA. This biological contribution to INP at higher temperatures is important for subsequent cloud development. The temperature range where simulated INP_{PBAP} exhibit considerable concentrations (1 L^{-1}, < -12°C) aligns closely with the temperature range where secondary ice is expected to be active -5°C to -20°C (Korolev and Leisner, 2020), with peak impact around ~15°C (Georgakaki et al., 2022). Although not contributing significant primary ice particles, INP_{PBAP} at warmer freezing temperatures may help sustain high concentrations of secondary ice, by contributing primary ice necessary for SIP. That said, SIP is most effective for situations where there are seeder-feeder cloud configurations (i.e., layered clouds or vertically developed clouds that have internal seeding; Georgakaki and Nenes, 2023) so it remains to be investigated whether the "niche" impact of INP from PBAP on SIP is climatically important.

To illustrate the various components of INP depending on atmospheric temperature, figure 3 presents the INP total number concertation column (up to 300 hPa) sampled from the model results for three different air temperature ranges [-40 °C to -30 °C (Fig. 3a), -30 °C to -20 °C (Fig. 3b) and -20 °C to -10 °C (Fig. 3c)]. We also present the annual mean percentage contribution from mineral dust, MPOA and PBAP for these columns. Figure 3 clearly shows that PBAP are the main INP precursor in temperatures ranging from -20°C to -10°C in both hemispheres while MPOA and mineral dust are the primary source of INP at lower temperatures. Additionally, for temperature range between -40 °C to -30 °C (Fig. 3a) and -30 °C to -20 °C (Fig. 3b) mineral dust emerges as the dominant source of INP (more than 90%) in NH while MPOA are the main source in SH (more than 75%).

The zonal distribution of INP exhibits a notable altitude dependent variation in the contribution of INP precursors. As discussed, INP_D dominate at high altitudes, whereas INP_{PBAP} and INP_{MPOA} dominate at low altitudes. Figure 4 provides a comprehensive insight into the global contribution of distinct INP sources and establishes a correlation between the percentage contribution of each INP type and the concentration ranges of INP. The INP column burdens (m^{-2}) from surface up to 600 hPa (Fig. 4a) and up to 300 hPa (Fig. 4b) are depicted, along with the seasonal percentage contribution of the three different types of INP in the SH and NH. The INP column up to 600 hPa (Fig. 4a) reveals that mineral dust is the dominant INP precursor in the NH during boreal winter and spring (DJF, MAM), accounting for ~75% on average. During summer and autumn (JJA, SON), PBAP emerges as the primary source of INP, which strongly correlates with vegetation growth, as aforementioned. The contribution of MPOA remains minor across all seasons, accounting for

~~almost 10%. In contrast, in the SH, the dominant source of INP is MPOA (about 83 % of the INP column up to 600 hPa), followed by dust (about 17%), while the contribution of PBAP is almost negligible (about 2.5%). However, it should be noted that in equatorial regions where the major sources of PBAP are located, ice nucleation occurs at pressures lower than 600 hPa. This explains the small contribution of PBAP up to 600hPa.~~

~~The INP column burden up to 300 hPa is depicted in Figure 4b. Mineral dust serves as the predominant INP precursor in the NH across all seasons (at least 50%), accounting for 68% of the column on annual average. INP_{PBAP} represents ~27% of the INP column, with an increased contribution during the boreal summer and fall months (~45%). The contribution of INP_{MPOA} is small, about 5%. Conversely, the major contributor to the INP population in the SH is MPOA, representing on annual average approximately 46% of the total INP column. It is followed by INP_{PBAP} at about 30%, which is maximized in the austral summer (DJF, 35%), while mineral dust plays a comparatively minor role, contributing ~24%. This is partly attributed to the low fraction of K-feldspar minerals estimated to be present in dust particles emitted from the Patagonian and the Kalahari Deserts (Journet et al., 2014; Nickovic et al., 2012). The amount of simulated INP is~~ greater in the NH than in the SH, which is in agreement with previous studies (Vergara-Temprado et al., 2017). Figure 8b shows the associated interannual variability of the simulated INP multiyear mean columns indicated by the coefficient of variation that is calculated as the standard deviation of the annual mean columns to the multiyear annual mean and is expressed in percent. We find that locally the interannual variability can exceed 150%, particularly in the tropics and the polar regions and has to be kept in mind when interpreting modeling results. Figure 8c shows that mineral dust is the dominant source of INP in the high northern latitudes (60°-90°N) across all seasons, with contributions exceeding 89% in every season. INP_{PBAP} and INP_{MPOA} play minimal roles, with INP_{PBAP} contribution to the column burden of the total INP peaking at about 8.5% in the fall (SON). In mid-latitudes and the tropics (60°S-60°N), INP contributions are more seasonally variable, highlighting the interplay between dust and biological particles in this region. Mineral dust dominates during MAM (spring NH) and SON (autumn NH), while INP_{PBAP} plays a prominent role in DJF (winter NH), contributing about 65%. In the high southern latitudes (60-90°S), mineral dust remains the main source of INP, especially in DJF (summer SH), where it accounts for about 82.5%. However, in contrast to the other latitude zones, INP_{MPOA} shows significant contributions to the total INP column burden in MAM (about 37%) and JJA (about 31.5%) in this latitude zone, while INP_{PBAP} contribution is negligible.

[FIGURE8]

To further illustrate the different components of ambient INP depending on atmospheric temperature, Figure 9 presents the percent contributions of INP types calculated at modelled ambient temperature and classified in three temperature ranges: [-40°C, -30°C], [-30°C, -20°C], and [-20°C, -10°C]. The figure highlights the spatial variability as a function of temperature of the contribution of the studied species to the total simulated

INP at the modelled ambient temperature. In order to plot this figure, all model results are selected for which the modelled temperature falls within the respective temperature range. The percent contributions of each INP type to the total INP in each of the model grids and instances are calculated and then averaged per model grid, for all altitudes. According to our simulations, mineral dust contributes significantly at all temperatures, especially below -20ºC, where its influence is widespread, and maximizes over desert areas such as the Sahara. At the coldest temperature range (-40°C to -30°C), dust dominates globally, extending its influence over oceanic regions even in the SH. At this temperature range MPOA contribution is apparent mainly in the Southern Ocean high latitudes but also in the tropical Pacific, while PBAP contribution to INP is negligible.

[FIGURE 9]

In the middle temperature range (-30°C to -20°C) dust remains the dominant INP type, while PBAP contribution to INP becomes apparent over land. MPOA remains relevant in the tropical Pacific and the Southern Ocean. At higher temperatures (-20°C to -10°C), PBAP becomes the dominant INP type in tropical and subtropical regions, while MPOA dominates over the Southern Ocean (60°S–90°S), where it accounts for nearly 90% of the total INP, highlighting the strong influence of marine aerosols in polar ocean regions. In this temperature range, dust INP contributes mainly to total INP in high latitudes of the NH (e.g., the Arctic).

The recent observational study by Creamean et al. (2022) in the central Arctic revealed a strong seasonality of INP during the year, with lower concentrations in winter and spring controlled by transport from lower latitudes, and enhanced concentrations of INP in summer, likely of marine biological origin. This only partially agrees with our results, which show that INP concentrations in the Arctic region are mainly influenced by transported airborne dust in winter and spring, by INP_{PBAP} in summer and fall and that INP_{PBAP} contributes more than INP_{MPOA} in summer (Fig. S2). ~~Figure 5(a-c) depicts the simulated distributions of INP derived from each studied aerosol type present at ~600 hPa and with the ability to freeze at ~20°C in immersion mode (hereafter called INP_{-20}). These conditions of temperature and pressure are representative of MPC's glaciation and allow all species to activate and act as INP. In addition, the simulation of INP concentration at specific temperatures (e.g., ~20ºC) is required to compare modelled and observed INP concentrations, since the measurements of INP concentrations are determined by exposing particles to controlled temperatures within the instrumentation. Figure 5d shows the total INP distribution calculated accounting for all the aforementioned tracers.~~

~~The concentrations of INP_{D-20} (Fig. 5a) contribute much more to mid-latitude INP concentrations in the NH than in the SH due to long-range atmospheric transport patterns from sources that favour dust present in the NH. Throughout much of the low and mid-latitudes of the NH, INP_{D-20} outnumbers by far $INP_{MPOA-20}$ and~~

~~$INP_{PBAP\text{-}20}$ (Fig.~~ This discrepancy may be due to the underprediction of MPOA and overprediction of PBAP and dust concentrations discussed in Sect. 3.1.2.

Comparison of INP~~5a-e). $INP_{MPOA\text{-}20}$ dominates in the oceanic regions, in particular those in the SH, and $INP_{PBAP\text{-}20}$ prevails over tropical and equatorial continental sites and up to +/- 40º latitude. However, there are oceanic regions in the South Atlantic Ocean (such as the West coast of S. Africa and the North west coast of S. America) where PBAP has the potential to form ice crystals at the outflow of the continental air (Fig. 5b) and in the middle and high troposphere (Fig. 2e), enhancing INP concentrations in marine environments.~~

3.2.3 ~~3.2 Comparing~~ predictions with observations

Cloud-resolved high-resolution ~~modeling~~modelling studies indicate that clouds can present sensitivity to INP perturbations that exceed one order of magnitude (Fan et al., 2017). For the simulation of INP in models to be deemed satisfactory, prediction errors must be constrained to less than an order of magnitude for the majority of observations (Cornwell et al., 2023). Figure ~~6~~10 shows the comparison of INP observations with simulated INP, for each INP ~~precursor~~type separately and for all possible combinations. ~~Two metrics~~All observations were compared with spatiotemporally co-located simulated concentrations, except observations out of the simulation window, which were compared with climatological monthly mean geographically co-located model results. The Pt_1, $Pt_{1.5}$ and the correlation coefficient (R) defined in Sect.2.4 are used to assess the ability of the model to correctly predict INP concentrations for each of the depicted cases and are reported in this ~~Figure: i) the percentage of INP simulated values within one order of magnitude from the observed values (Pt_1) and ii) the percentage within one and half orders of magnitude ($Pt_{1.5}$). The correlation between observed and predicted INP is presented by the correlation coefficient (R).~~figure.

[FIGURE 10]

Considering dust minerals as the sole INP ~~precursors~~types leads to underestimation against observations (Fig. ~~6a~~10a; Pt_1 about 24% and R=0.84). Even if dust is the most abundant aerosol in the atmosphere, the simulated dust-derived INP cannot predict the observed INP, especially at high temperatures (>-15ºC~~). Mineral~~) and relatively low INP levels, since mineral dust particles likely become ice-active only at low temperatures (Chatziparaschos et al., 2023; Cornwell et al., 2023). Notably, the results show that there is some overestimation for colder temperatures, which may be partly related to the overestimation of dust in the model. Findings in agreement with the literature (e.g. Vergara-Temprado et al., 2018) and our earlier study by Chatziparaschos et al. (2023). ~~However, there are large uncertainties in this hypothesis since dust minerals may be carriers of biogenic ice-active matter (Hill et al., 2016; O'Sullivan et al., 2016), which enhances dust nucleation activity at higher temperatures. The existence of PBAP onto mineral dust and their effect on its~~

~~ice nucleating activity requires dedicated studies and improved parameterizations. These findings are largely in agreement with the literature and have been thoroughly discussed in Chatziparaschos et al. (2023).~~

~~INP_{MPOA} alone significantly improves the prediction of the observed INP at high temperatures, increasing the predictability of the model to 70% (Pt_1, Fig. 6b). However, this improvement is accompanied by a decrease in correlation coefficient (R). At low (< 30°C) and mid (-20°C) temperatures INP_{MPOA} underestimates the observations (Fig. 6b). The discrepancy between observed INP and INP_{MPOA} estimated from the Wilson et al. (2015) relationship may suggest a deficiency in the relationship used between Chl a concentrations and MPOA emissions (McCluskey et al., 2017). In addition, it has been previously reported by McCluskey et al. (2018) that the Wilson et al. (2015) parameterization may overpredict INP. Nevertheless, our findings do not support this outcome. The model results tend to slightly overpredict INP only in the temperature range around -25 °C. Wilson et al. (2015) identified a temperature-dependent relationship between total organic carbon mass and ice nucleating entity (Vali et al., 2015) number concentrations in sea surface microlayer samples, while the McCluskey et al. (2018) parameterization has no explicit dependence on the organic carbon content of SS. The Wilson et al. (2015) parameterization was empirically derived from observations of ambient SS, proposing ice nucleation site densities (INP per square meter of aerosol) associated with SS surface area. This approach requires the quantification of SS size distributions and detailed organic composition, taking into account the SS size variability that occurred due to marine biological processes; this process is not parameterized in McCluskey et al. (2018). However, there is clear evidence of the link between marine organic matter and INP activity (McCluskey et al., 2017, 2018; Wilson et al., 2015) and both the amount and the composition of organic components included in the SS are a strong function of particles size (Wang et al., 2017; O'Dowd et al., 2004). Therefore, our model, which calculates INP using the Wilson et al. (2015) parameterization and accounts for the MPOA mass dependence on the presence of Chl a (Vignati et al., 2010) and for the MPOA ageing process (section 2.2), may provide a more realistic approach. These findings indicate that the representation of SS significantly influences INP, emphasizing the need for future studies to accurately quantify sea spray size distributions and detailed organic composition.~~

~~Figure 6c~~INP_{MPOA} alone significantly improves the prediction of the observed INP at high temperatures, increasing the predictability of the model from about 24% for dust alone to about 65% for MPOA alone (Pt_1, Figs. 10a and 10b). However, this improvement is accompanied by a decrease in the correlation coefficient (R). At low (<-30°C) and mid (-20°C) temperatures, INP_{MPOA} underestimates the observations (Fig. 10b). The discrepancy between observed INP and INP_{MPOA} can be partially attributed to missing INP sources, especially dust, and partially to the uncertainty in the INP_{MPOA} simulations resulting from both the MPOA simulations and the INP_{MPOA} parameterization.

Figure10c shows the comparison between simulated INP_{PBAP} and observed INP. INP_{PBAP} overestimate the observed INP across temperature ranges warmer than -30°C, followed by a subsequent underestimation ~~beyond~~below this temperature. The model's predictability increases (Pt_1 = ~~61~~60%) compared to INP_D (Pt_1 =

~~51~~24%) but decreases compared to INP_{MPOA} (Pt_1 ~~~~70~~65%). This~~ overall~~ overestimation could be attributed to uncertainties in parameterizations for PBAP emissions and for the ice nuclei activity of PBAP~~ or to our~~. Since a 20% overestimation of PBAP concentrations by the model ~~performance. It has been proved~~can be deduced when compared to observations, an overestimation of the INP scheme seems to be the most plausible reason for the INP_{PBAP} overestimation.

The deviation of simulated individual INP types from observations, shown in Figure S6 as a function of binned temperatures, indicates that at temperatures of about -25 to -30°C, both INP_D and INP_{PBAP} separately overestimate the observed INP. For warmer temperatures, Figure S6 shows that a major contribution to the model overestimation of the observed total INP is due to INP_{PBAP}. Overall, among the three different types of INP when considered individually, the highest correlation (r =0.84, Fig. 10a) between simulated and observed INP concentrations is found for INP_D, which however fails to reproduce the low levels of INP at relatively warm temperatures.

When considering all INP types, the model's agreement with the INP observations is moderate, with a correlation coefficient of 0.86 and about 59% (Pt_1) predictability (Fig. 10f). Considering only INP from MPOA in addition to dust improves the predictive ability of the model (about 71%, Pt_1) and has the highest correlation coefficient of 0.88 (Fig. 10d). The inclusion of MPOA improves the model's comparison between -6°C and -25°C where MPOA exhibits high ice activity. Including INP_{PBAP} in the simulations in addition to INP_D and INP_{MPOA} leads to an overprediction of INP measurements and reduces the accuracy of the model's predictions (Fig. 10f).

However, as seen in Figure S7, INP_{PBAP} compares well with INP observations in the NH and the extratropical SH (Figure S7 top and mid-rows). Therefore, in no case our results should diminish the role of INP derived from PBAP, especially in regions where PBAP is more abundant or ecosystems are diverse, such as the Amazon, affecting INP concentrations locally (Prenni et al., 2009). Most of the INP at warmer temperatures than -16°C are bioaerosols, suggesting that without improved representations of the sources and ice-nucleating activities of biological INP, models will struggle to simulate total INP concentrations at warmer temperatures and the resulting MPC.

3.3 Sources of uncertainties and implications for our results.

Earth System Models (ESM) encounter significant radiation biases mainly in remote marine regions away from major INP sources, where the prevalence of MPOA results in low INP concentrations (Vergara-Temprado et al., 2018). ~~laboratory~~McCluskey et al. (2018) have reported that the Wilson et al. (2015) parameterization for MPOA ice activity may overpredict INP_{MPOA}. Our model tends to slightly underpredict INP in the temperature range around -25°C, consistent with the earlier discussed underprediction of MPOA levels by the model. Thus, the overly active parameterization of Wilson et al. (2015), shown by McCluskey et al. (2018), may be counteracting the model's underestimation of MPOA.

Our results suggest that for climate prediction, with the current knowledge of ice nuclei properties of dust, PBAP and MPOA and as a first approximation, consideration of mineral dust and MPOA as the main contributors to INP globally could be sufficient, although PBAP regionally and at warm temperatures is an important contributor to INP. However, there are large uncertainties associated with these results related both with the number concentrations of the various INP types and with the ice nucleating activity of the INP relevant aerosols. Parameterizations and model evaluation are based on observations geographically and temporally limited and used for global estimates; therefore, their global applicability remains an open issue. In Section 3.1.2, we evaluated the uncertainties in the simulated dust, MPOA, and PBAP concentrations by comparisons with available observations and found significant overprediction of dust (~ 60%) and PBAP (~ 20%) and underprediction of MPOA (3% to 50%).

The uncertainties in the simulation of INP number concentrations combine the biases in the INP-relevant aerosol simulations with those of the parameterizations of the INP activity of different types of aerosols. Laboratory studies proved that the ice nuclei activity of bacterial and fungal spores can vary substantially across different species (Pummer et al., 2012; Murray et al., 2012). The species composition of airborne fungal and bacterial communities exhibits considerable geographic variability (Dietzel et al., 2019). Thus, it is reasonable to expect that the ice nucleating efficiency of airborne PBAP may strongly differ geographically. ~~The~~In addition, the INP parameterizations ~~we have~~ used here were developed based on a small number of samples from the mid-latitudinal ponderosa pine forest ecosystem (Tobo et al., 2013) and ~~may not be representative of the global simulation of INP_{PBAP}. On the other hand, our model is able to simulate the mean number and mass concentrations of PBAP within the correct order of magnitude, and seasonal cycles and regional scale geographic distributions that correlate with observed patterns; however, it slightly overestimates the BCT and FNG burden, as reported by Myriokefalitakis et al. (2017). This could impact the simulated INP_{PBAP}, contributing to this observed overestimation. Overall, among the three different types of INP when considered individually the highest correlation is found for INP_D~~thus may not be representative of the global simulation of INP_{PBAP}.

Furthermore, INP dust parameterizations can introduce significant biases in the calculations: INP_D simulations by CAM6 model were found to vary by a factor of 2 at temperatures lower than −25°C when two different parameterizations were used (McCluskey et al., 2023) with the one overpredicting INP from dust aerosol. Given the significant differences in freezing efficiency between marine and dust aerosols, simulated dust concentrations play a critical role in influencing study results, particularly in marine regions. An overestimation of INP_D could mask the potential effect of other INP types on cloud properties.

Dust particles typically have ice nucleating activities up to two to three orders of magnitude greater than marine particles at the same temperature (Cornwell et al., 2023; McCluskey et al., 2018). However, there are large uncertainties in this hypothesis since dust minerals may be carriers of biogenic ice-active matter (Hill et al., 2016; O'Sullivan et al., 2016), which would enhance dust nucleation activity at higher temperatures.

The existence of PBAP on mineral dust or dust coating by pollutants during the atmospheric ageing of dust (Iwata and Matsuki, 2018) and their effect on its dust nucleating activity require dedicated studies and improved parameterizations. More generally, the co-existence, as internal mixing, of the various INP types has not been studied and could lead to an enhancement or reduction of the ice activity of the particles. In addition, atmospheric processes, such as the ageing of aerosols, can lead to the degradation of ice-nucleation activity. For instance, ageing with sulfuric acid can either greatly reduce the immersion mode ice-nucleation activity or have little effect (Kumar et al., 2019a, b; Jahl et al., 2021), while ammonium salts can cause suspended particles of K-feldspar and quartz to nucleate ice at substantially higher temperatures than they do in pure water (Whale et al., 2018). Although there are conflicting findings and limited understanding regarding how to parameterize the ice-nucleation activity of aged particles, potential ageing effects directly on INP are not considered in our study. The effects of atmospheric ageing on ice-nucleating activity are probably a minor source of error in this study, in comparison to the introduced bias from the employed INP parameterizations and model performance~~The model's agreement with the INP observations is moderate, with a correlation coefficient of 0.87 and about 59% (Pt_1) predictability when considering all INP types (Fig. 6f). Considering only mineral dust and MPOA (Fig. 6d) improves the predictive ability of the model (about 73%, Pt_1) and has the highest correlation coefficient 0.88 (Fig. 6e~~ in simulating INP-relevant particles. The results presented in this study, and particularly the relative importance of various INP types, which is discussed assuming externally mixed INP, have to be revisited when additional information of the mixing of INP types and how this affects the overall properties of the INP become available.

In summary, the comparison of model results with observations reveals that dust particles are a minor INP source at warm temperatures~~). The inclusion of MPOA improves the model's comparison between -6°C and -25°C where MPOA exhibits high ice activity. Model results are more consistent with observations, with the model reproducing about 73% of observations within an order of magnitude and about 87% within one and a half orders of magnitude, as illustrated in Figure 6d. These findings suggest that for climate prediction, with the current knowledge of ice nuclei properties of dust, PBAP and MPOA, consideration of mineral dust and MPOA as the main contributor to INP globally could be sufficient. Dust particles typically have ice nucleating activities up to two to three orders of magnitude greater than marine particles at the same temperature (Cornwell et al., 2023; McCluskey et al., 2018); however the INP_{MPOA} concentration depends on the location and the altitude of the measurements. Marine particles are an important source of INP at locations distant from land. Including INP_{PBAP} in the simulations in addition to INP_D and INP_{MPOA} leads to an overestimation of measurements and reduces the accuracy of the model's predictions (Fig. 6f). In no case should this~~ diminish the role of INP derived from PBAP, especially in regions where PBAP is more abundant or ecosystems are diverse, such as the Amazon, affecting INP concentrations locally (Prenni et al., 2009). ~~Most of the INP at warmer temperatures than -16°C are bioaerosols, suggesting that without improved representations of the sources and ice-nucleating activities of biological INP, models will struggle to simulate total INP concentrations at warmer temperatures and the resulting MPC.~~

~~Other sources of model bias may be attributed to atmospheric processes, such as the ageing of aerosols that results in the degradation of ice-nucleation activity. For instance, ageing with sulfuric acid can either greatly reduce the immersion mode ice nucleation activity or have little effect (Kumar et al., 2019a, b; Jahl et al., 2021). Although there are conflicting findings and limited understanding regarding how to parameterize the ice-nucleation activity of aged particles, potential ageing effects directly on INP are not considered in our study. The effects of atmospheric ageing on ice-nucleating activity are probably a minor source of error in this study, in comparison to the introduced bias from the employed INP parameterizations and model performance.~~

~~In summary, the comparison of model results with observations reveals that dust particles are a minor INP source at warm temperatures,~~ but increase in importance at colder temperatures. INP at temperatures in the vicinity of zero (warmer than -20°C) are typically related to INP from biogenic sources~~.~~, as simulated by PBAP and MPOA. These findings are consistent with previous observational studies showing that biological INP make up a greater fraction of continental~~-~~ INP at warm temperatures (Mason et al., 2015; Gong et al., 2022). The model achieves its highest predictability and correlation against observed INP across all temperature ranges when both INP_D and INP_{MPOA} are included~~.~~, but the overprediction of dust aerosol suggests the need to additionally account for INP_{PBAP} in climate modeling.

4 Conclusions

In this study, we performed global model simulations of mineral dust, primary marine organic aerosols, and terrestrial ~~bioaerosol~~bioaerosols (bacterial and fungal spores) and investigated their contribution to atmospheric ice nucleation using laboratory-derived parameterizations based on the singular description approach. At relatively warm temperatures (warmer than −20 °C), the majority of INP are typically of biological origin, while at lower temperatures and higher altitudes, INP from mineral dust dominates globally. INP from dust contributes more to total INP in the mid-latitudes in the NH than in the SH due to the location of the dust sources and the long-range atmospheric transport patterns. INP from terrestrial bioaerosol peaks in the low and mid-troposphere and could be important in reproducing/representing atmospheric INP populations at warm temperatures. ~~Concentrations~~ Simulated concentrations of INP from terrestrial bioaerosol vary ~~depending on the~~ with season and ~~regional weather patterns.~~meteorological factors that affect both the source of PBAP and its ability to act as INP. INP from terrestrial bioaerosol has the potential to form ice crystals in the ~~NH~~ subtropics at the outflow of ~~the~~ continental air. Simulated INP from marine bioaerosol ~~are~~is found primarily ~~found~~ over oceans and coastal areas and ~~dominate~~dominates between 40°-90°S (Southern Ocean), with high concentrations in regions of high sea spray and phytoplankton activity that influence the source of MPOA.

The model achieves its highest predictability against observed INP across all temperature ranges when both INP_D and INP_{MPOA} are included. Further inclusion of PBAP in our model leads to an overestimation of the measurements~~.~~, which might indicate an overestimation of the INP scheme for PBAP. Our study suggests that INP_D and INP_{MPOA} could sufficiently predict observed INP concentrations globally. However, bioaerosols are an important source of warm-temperature INP, affecting mainly ~~at~~ low altitudes.

~~Therefore, we propose a scheme designed to predict INP global distribution based on the most influential precursors for in-cloud ice initiation, namely mineral dust, MPOA and PBAP. The current model biases could~~The current model biases can likely be attributed to the uncertainties in the parameterizations for the ice-nucleating activity of each particle type, simplified source functions for particle emissions, and description of aerosol transport. Uncertainties exist, particularly ~~with regard to~~regarding the impact of atmospheric mixing and processing of different INP species on INP properties. For instance, dust minerals could be carriers of biogenic ice-active macromolecules and bioaerosol ~~—~~or be coated by sulphate and/or nitrate or other pollutants during the atmospheric ageing of dust ~~(Iwata and Matsuki, 2018).~~. These processes are at present neglected or heavily parameterized in our model and could lead to the enhancement or reduction of INP ice-activation properties. ~~For example, ammonium salts can cause suspended particles of feldspars and quartz to nucleate ice at substantially higher temperatures than they do in pure water (Whale et al., 2018). Conversely, sulfate acids can dramatically depress freezing for the aforementioned nucleators. Future studies should~~Future studies should also investigate the impact of atmospheric mixing and ageing on INP concentrations and constrain them by measurements over receptor areas downwind of source regions. Due to the large variability of INP with space and time, effort must be put into acquiring more data on INP ambient levels as well as the ice nucleating properties of individual aerosol types as well as how these change with atmospheric ageing. These are needed to build regionally and globally representative datasets and reduce the uncertainty in the parameterizations of their sources in numerical models. Tackling these research priorities is essential for developing a more comprehensive understanding of the atmospheric variability of INP and their impacts in different cloud regimes and climate.

Acknowledgements. This work has been supported by the European Union Horizon 2020 project FORCeS under grant agreement No 821205. The early stages of this work have been supported by the project "PANhellenic infrastructure for Atmospheric Composition and climatE change" (PANACEA; MIS 5021516), which is implemented under the Action "Reinforcement of the Research and Innovation Infrastructure", funded by the Operational Programme "Competitiveness, Entrepreneurship and Innovation" (NSRF 2014-2020) and co-financed by Greece and the European Union (European Regional Development Fund). ND, MK and MV acknowledge support from the Deutsche Forschungsgemeinschaft (DFG) under Germany´s Excellence Strategy (University Allowance, EXC 2077, University of Bremen). CPG-P, MC-S, MGA, and MC acknowledge support from the European Research Council under the European Union's Horizon 2020 research and innovation programme (grant n. 773051; FRAGMENT), the Horizon Europe

programme (Grant Agreement No 101137680 via project CERTAINTY) and from the AXA Research Fund. MC-S has received funding from the European Union's Horizon 2020 research and innovation programme, under the Marie Skłodowska-Curie grant agreements, reference 754433 from the call H2020-MSCA-COFUND-2016. AN acknowledges support from project PyroTRACH (ERC-2016-COG) funded from H2020-EU.1.1. - Excellent Science - European Research Council (ERC), project ID 726165. SM and MK acknowledge support from the REINFORCE research project implemented in the framework of H.F.R.I call "Basic research Financing (Horizontal support of all Sciences)" under the National Recovery and Resilience Plan "Greece 2.0" funded by the European Union — Next Generation EU (H.F.R.I. Project Number: 15155).

Author contributions. MK and ~~MC~~MCh conceived the study. ~~MC~~MCh modified the model to account for INP and performed the simulations, visualized and analyzed data, and wrote the initial version of the paper. SM provided the initial code for bioaerosols of the model. MK supervised the work with feedback from AN and CPG-P and MK and CPG-P re-edited the paper. All authors provided scientific feedback contributed to the review and guidance, commented and provided revisions in subsequent versions editing of the paper before submission.

~~**Competing interests. Some authors are members of the editorial board of journal Atmospheric Chemistry and Physics.**~~

Data availability. The modeling data used for this analysis are available at 10.5281/zenodo.14041390

References

Ansmann, A., Tesche, M., Althausen, D., Müller, D., Seifert, P., Freudenthaler, V., Heese, B., Wiegner, M., Pisani, G., Knippertz, P., and Dubovik, O.: Influence of Saharan dust on cloud glaciation in southern Morocco during the Saharan Mineral Dust Experiment, J. Geophys. Res., 113, D04210, https://doi.org/10.1029/2007JD008785, 2008.

Arimoto, R., Duce, R. A., Ray, B. J., Ellis, W. G., Cullen, J. D., and Merrill, J. T.: Trace elements in the atmosphere over the North Atlantic, J. Geophys. Res., 100, 1199–1213, https://doi.org/10.1029/94JD02618, 1995.

Atkinson, J. D., Murray, B. J., Woodhouse, M. T., Whale, T. F., Baustian, K. J., Carslaw, K. S., Dobbie, S., O'Sullivan, D., and Malkin, T. L.: The importance of feldspar for ice nucleation by mineral dust in mixed-phase clouds., Nature, 498, 355–8, https://doi.org/10.1038/nature12278, 2013.

Augustin-Bauditz, S., Wex, H., Kanter, S., Ebert, M., Niedermeier, D., Stolz, F., Prager, A., and Stratmann, F.: The immersion mode ice nucleation behavior of mineral dusts: A comparison of different pure and surface modified dusts, Geophys. Res. Lett., 41, 7375–7382, https://doi.org/10.1002/2014GL061317, 2014.

Augustin-Bauditz, S., Wex, H., Denjean, C., Hartmann, S., Schneider, J., Schmidt, S., Ebert, M., and Stratmann, F.: Laboratory-generated mixtures of mineral dust particles with biological substances: characterization of the particle mixing state and immersion freezing behavior, Atmos. Chem. Phys., 16, 5531–5543, https://doi.org/10.5194/acp-16-5531-2016, 2016.

Bauer, H., Schueller, E., Weinke, G., Berger, A., Hitzenberger, R., Marr, I. L., and Puxbaum, H.: Significant contributions

of fungal spores to the organic carbon and to the aerosol mass balance of the urban atmospheric aerosol, Atmos. Environ., 42, 5542–5549, https://doi.org/10.1016/j.atmosenv.2008.03.019, 2008.

Bigg, E. K.: Ice Nucleus Concentrations in Remote Areas, J. Atmos. Sci., 30, 1153–1157, https://doi.org/10.1175/1520-0469(1973)030<1153:INCIRA>2.0.CO;2, 1973.

Bigg, E. K.: Long-term trends in ice nucleus concentrations, https://doi.org/10.1016/0169-8095(90)90025-8, 1990.

Billault-Roux, A.-C., Georgakaki, P., Gehring, J., Jaffeux, L., Schwarzenboeck, A., Coutris, P., Nenes, A., and Berne, A.: Distinct secondary ice production processes observed in radar Doppler spectra: insights from a case study, Atmos. Chem. Phys., 23, 10207–10234, https://doi.org/10.5194/acp-23-10207-2023, 2023.

Bodas-Salcedo, A., Hill, P. G., Furtado, K., Williams, K. D., Field, P. R., Manners, J. C., Hyder, P., and Kato, S.: Large Contribution of Supercooled Liquid Clouds to the Solar Radiation Budget of the Southern Ocean, J. Clim., 29, 4213–4228, https://doi.org/10.1175/JCLI-D-15-0564.1, 2016.

Bones, D. L., Henricksen, D. K., Mang, S. A., Gonsior, M., Bateman, A. P., Nguyen, T. B., Cooper, W. J., and Nizkorodov, S. A.: Appearance of strong absorbers and fluorophores in limonene-O 3 secondary organic aerosol due to ~~NH 4~~ NH_4^+ -mediated chemical aging over long time scales, J. Geophys. Res. Atmos., 115, 1–14, https://doi.org/10.1029/2009JD012864, 2010.

Boose, Y., Welti, A., Atkinson, J., Ramelli, F., Danielczok, A., Bingemer, H. G., Plötze, M., Sierau, B., Kanji, Z. A., and Lohmann, U.: Heterogeneous ice nucleation on dust particles sourced from nine deserts worldwide – Part 1: Immersion freezing, Atmos. Chem. Phys., 16, 15075–15095, https://doi.org/10.5194/acp-16-15075-2016, 2016.

Boose, Y., Baloh, P., Plötze, M., Ofner, J., Grothe, H., Sierau, B., Lohmann, U., and Kanji, Z. A.: Heterogeneous ice nucleation on dust particles sourced from nine deserts worldwide - Part 2: Deposition nucleation and condensation freezing, Atmos. Chem. Phys., 19, 1059–1076, https://doi.org/10.5194/acp-19-1059-2019, 2019.

Borys, R. D., Lowenthal, D. H., Cohn, S. A., and Brown, W. O. J.: Mountaintop and radar measurements of anthropogenic aerosol effects on snow growth and snowfall rate, Geophys. Res. Lett., 30, https://doi.org/https://doi.org/10.1029/2002GL016855, 2003.

Burrows, S. M., Butler, T., Jöckel, P., Tost, H., Kerkweg, a., Pöschl, U., and Lawrence, M. G.: Bacteria in the global atmosphere – Part 2: Modelling of emissions and transport between different ecosystems, Atmos. Chem. Phys. Discuss., 9, 10829–10881, https://doi.org/10.5194/acpd-9-10829-2009, 2009.

Burrows, S. M., Hoose, C., Pöschl, U., and Lawrence, M. G.: Ice nuclei in marine air: Biogenic particles or dust?, Atmos. Chem. Phys., 13, 245–267, https://doi.org/10.5194/acp-13-245-2013, 2013.

Burrows, S. M., McCluskey, C. S., Cornwell, G., Steinke, I., Zhang, K., Zhao, B., Zawadowicz, M., Raman, A., Kulkarni, G., China, S., Zelenyuk, A., and DeMott, P. J.: Ice-Nucleating Particles That Impact Clouds and Climate: Observational and Modeling Research Needs, https://doi.org/10.1029/2021RG000745, 16 June 2022.

Chatziparaschos, M., Daskalakis, N., Myriokefalitakis, S., Kalivitis, N., Nenes, A., Gonçalves Ageitos, M., Costa-Surós, M., Pérez ~~Gare\'\ia~~Garcia-Pando, C., Zanoli, M., Vrekoussis, M., and Kanakidou, M.: Role of K-feldspar and quartz in global ice nucleation by mineral dust in mixed-phase clouds, Atmos. Chem. Phys., 23, 1785–1801, https://doi.org/10.5194/acp-23-1785-2023, 2023.

Chen, J., Wu, Z., Chen, J., Reicher, N., Fang, X., Rudich, Y., and Hu, M.: Size-resolved atmospheric ice-nucleating particles during East Asian dust events, Atmos. Chem. Phys., 21, 3491–3506, https://doi.org/10.5194/acp-21-3491-2021, 2021.

Choi, Y.-S., Ho, C.-H., Park, C.-E., Storelvmo, T., and Tan, I.: Influence of cloud phase composition on climate feedbacks, J. Geophys. Res. Atmos., 119, 3687–3700, https://doi.org/10.1002/2013JD020582, 2014.

Chubb, T. H., Jensen, J. B., Siems, S. T., and Manton, M. J.: In situ observations of supercooled liquid clouds over the Southern Ocean during the HIAPER Pole-to-Pole Observation campaigns, Geophys. Res. Lett., 40, 5280–5285, https://doi.org/10.1002/grl.50986, 2013.

Claquin, T., Schulz, M., and Balkanski, Y. J.: Modeling the mineralogy of atmospheric dust sources, J. Geophys. Res. Atmos., 104, 22243–22256, https://doi.org/10.1029/1999JD900416, 1999.

Cooke, W. F., Liousse, C., Cachier, H., and Feichter, J.: Construction of a 1° × 1° fossil fuel emission data set for carbonaceous aerosol and implementation and radiative impact in the ECHAM4 model, J. Geophys. Res. Atmos., 104, 22137–22162, https://doi.org/10.1029/1999JD900187, 1999.

Cornwell, G., McCluskey, C., Hill, T. C., Levin, E., Rothfuss, N., Tai, S.-L., Petters, M. D., DeMott, P. J., Kreidenweis, S., Prather, K., and Burrows, S. M.: Dataset for "Bioaerosols are the dominant source of warm-temperature immersion-mode INPs and drive uncertainties in INP predictability, https://doi.org/10.25584/1890223, 2022.

Cornwell, G. C., McCluskey, C. S., Hill, T. C. J., Levin, E. T., Rothfuss, N. E., Tai, S.-L., Petters, M. D., DeMott, P. J., Kreidenweis, S., Prather, K. A., and Burrows, S. M.: Bioaerosols are the dominant source of warm-temperature immersion-mode INPs and drive uncertainties in INP predictability, Sci. Adv., 9, eadg3715, https://doi.org/10.1126/sciadv.adg3715, 2023.

Costa, A., Meyer, J., Afchine, A., Luebke, A., Günther, G., Dorsey, J. R., Gallagher, M. W., Ehrlich, A., Wendisch, M., Baumgardner, D., Wex, H., and Krämer, M.: Classification of Arctic, midlatitude and tropical clouds in the mixed-phase temperature regime, Atmos. Chem. Phys., 17, 12219–12238, https://doi.org/10.5194/acp-17-12219-2017, 2017.

Creamean, J. M., Barry, K., Hill, T. C. J., Hume, C., DeMott, P. J., Shupe, M. D., Dahlke, S., Willmes, S., Schmale, J., Beck, I., Hoppe, C. J. M., Fong, A., Chamberlain, E., Bowman, J., Scharien, R., and Persson, O.: Annual cycle observations of aerosols capable of ice formation in central Arctic clouds, Nat. Commun., 13, 3537, https://doi.org/10.1038/s41467-022-31182-x, 2022.

Cziczo, D. J., Froyd, K. D., Hoose, C., Jensen, E. J., Diao, M., Zondlo, M. A., Smith, J. B., Twohy, C. H., and Murphy, D. M.: Clarifying the Dominant Sources and Mechanisms of Cirrus Cloud Formation, Science (80-.)., 340, 1320–1324, https://doi.org/10.1126/science.1234145, 2013.

D'Alessandro, J. J., Diao, M., Wu, C., Liu, X., Jensen, J. B., and Stephens, B. B.: Cloud Phase and Relative Humidity Distributions over the Southern Ocean in Austral Summer Based on In Situ Observations and CAM5 Simulations, J. Clim., 32, 2781–2805, https://doi.org/10.1175/JCLI-D-18-0232.1, 2019.

Dee, D. P., Uppala, S. M., Simmons, A. J., Berrisford, P., Poli, P., Kobayashi, S., Andrae, U., Balmaseda, M. A., Balsamo, G., Bauer, P., Bechtold, P., Beljaars, A. C. M., van de Berg, L., Bidlot, J., Bormann, N., Delsol, C., Dragani, R., Fuentes, M., Geer, A. J., Haimberger, L., Healy, S. B., Hersbach, H., Hólm, E. V., Isaksen, L., Kållberg, P., Köhler, M., Matricardi, M., Mcnally, A. P., Monge-Sanz, B. M., Morcrette, J. J., Park, B. K., Peubey, C., de Rosnay, P., Tavolato, C., Thépaut, J. N., and Vitart, F.: The ERA-Interim reanalysis: Configuration and performance of the data assimilation system, Q. J. R. Meteorol. Soc., 137, 553–597, https://doi.org/10.1002/qj.828, 2011.

DeMott, P. J. and Prenni, A. J.: New Directions: Need for defining the numbers and sources of biological aerosols acting as ice nuclei, Atmos. Environ., 44, 1944–1945, https://doi.org/10.1016/j.atmosenv.2010.02.032, 2010.

DeMott, P. J., Prenni, A. J., Liu, X., Kreidenweis, S. M., Petters, M. D., Twohy, C. H., Richardson, M. S., Eidhammer, T., and Rogers, D. C.: Predicting global atmospheric ice nuclei distributions and their impacts on climate., Proc. Natl. Acad. Sci., 107, 11217–22, https://doi.org/10.1073/pnas.0910818107, 2010.

Dietzel, K., Valle, D., Fierer, N., U'Ren, J. M., and Barberán, A.: Geographical Distribution of Fungal Plant Pathogens in Dust Across the United States, Front. Ecol. Evol., 7, 1–8, https://doi.org/10.3389/fevo.2019.00304, 2019.

Facchini, M. C., Decesari, S., Rinaldi, M., Carbone, C., Finessi, E., Mircea, M., Fuzzi, S., Moretti, F., Tagliavini, E., Ceburnis, D., and O'Dowd, C. D.: Important source of marine secondary organic aerosol from biogenic amines., Environ. Sci. Technol., 42, 9116–21, https://doi.org/10.1021/es8018385, 2008.

Fan, J., Ruby Leung, L., Rosenfeld, D., and Demott, P. J.: Effects of cloud condensation nuclei and ice nucleating particles on precipitation processes and supercooled liquid in mixed-phase orographic clouds, Atmos. Chem. Phys., 17, 1017–1035, https://doi.org/10.5194/acp-17-1017-2017, 2017.

Frey, W. R. and Kay, J. E.: The influence of extratropical cloud phase and amount feedbacks on climate sensitivity, Clim. Dyn., 50, 3097–3116, https://doi.org/10.1007/s00382-017-3796-5, 2018.

Genitsaris, S., Stefanidou, N., Katsiapi, M., Kormas, K. A., Sommer, U., and Moustaka-Gouni, M.: Variability of airborne bacteria in an urban Mediterranean area (Thessaloniki, Greece), Atmos. Environ., 157, 101–110, https://doi.org/10.1016/j.atmosenv.2017.03.018, 2017.

Georgakaki, P. and Nenes, A.: RaFSIP: Parameterizing ice multiplication in models using a machine learning approach, https://doi.org/10.22541/essoar.170365383.34520011/v1, 2023.

Georgakaki, P., Sotiropoulou, G., Vignon, É., Billault-Roux, A.-C., Berne, A., and Nenes, A.: Secondary ice production processes in wintertime alpine mixed-phase clouds, Atmos. Chem. Phys., 22, 1965–1988, https://doi.org/10.5194/acp-22-1965-2022, 2022.

Ginoux, P., Prospero, J. M., Torres, O., and Chin, M.: Long-term simulation of global dust distribution with the GOCART model: Correlation with North Atlantic Oscillation, Environ. Model. Softw., 19, 113–128, https://doi.org/10.1016/S1364-8152(03)00114-2, 2004.

Glaccum, R. A. and Prospero, J. M.: Saharan aerosols over the tropical North Atlantic — Mineralogy, Mar. Geol., 37, 295–321, https://doi.org/10.1016/0025-3227(80)90107-3, 1980.

Gong, S. L.: A parameterization of sea-salt aerosol source function for sub- and super-micron particles, Global Biogeochem. Cycles, https://doi.org/10.1029/2003GB002079, 2003.

Gong, X., Radenz, M., Wex, H., Seifert, P., Ataei, F., Henning, S., Baars, H., Barja, B., Ansmann, A., and Stratmann, F.: Significant continental source of ice-nucleating particles at the tip of Chile's southernmost Patagonia region, Atmos. Chem. Phys., 22, 10505–10525, https://doi.org/10.5194/acp-22-10505-2022, 2022.

Hande, L. B. and Hoose, C.: Partitioning the primary ice formation modes in large eddy simulations of mixed-phase clouds, Atmos. Chem. Phys., 17, 14105–14118, https://doi.org/10.5194/acp-17-14105-2017, 2017.

Harrison, A. D., Lever, K., Sanchez-Marroquin, A., Holden, M. A., Whale, T. F., Tarn, M. D., McQuaid, J. B., and Murray, B. J.: The ice-nucleating ability of quartz immersed in water and its atmospheric importance compared to K-feldspar, Atmos. Chem. Phys. Discuss., 1–23, https://doi.org/10.5194/acp-2019-288, 2019.

Heald, C. L. and Spracklen, D. V: Atmospheric budget of primary biological aerosol particles from fungal spores, Geophys. Res. Lett., 36, L09806, https://doi.org/10.1029/2009GL037493, 2009.

Hill, T. C. J., Demott, P. J., Tobo, Y., Fröhlich-Nowoisky, J., Moffett, B. F., Franc, G. D., and Kreidenweis, S. M.: Sources of organic ice nucleating particles in soils, Atmos. Chem. Phys., 16, 7195–7211, https://doi.org/10.5194/acp-16-7195-2016, 2016.

Hill, T. C. J., DeMott, P. J., Conen, F., and Möhler, O.: Impacts of Bioaerosols on Atmospheric Ice Nucleation Processes, in: Microbiology of Aerosols, Wiley, 195–219, https://doi.org/10.1002/9781119132318.ch3a, 2017.

Hofer, S., Hahn, L. C., Shaw, J. K., McGraw, Z. S., Bruno, O., Hellmuth, F., Pietschnig, M., Mostue, I. A., David, R. O., Carlsen, T., and Storelvmo, T.: Realistic representation of mixed-phase clouds increases projected climate warming, Commun. Earth Environ., 5, 390, https://doi.org/10.1038/s43247-024-01524-2, 2024.

Holden, M. A., Whale, T. F., Tarn, M. D., O'Sullivan, D., Walshaw, R. D., Murray, B. J., Meldrum, F. C., and Christenson, H. K.: High-speed imaging of ice nucleation in water proves the existence of active sites, Sci. Adv., 5, eaav4316, https://doi.org/10.1126/sciadv.aav4316, 2019.

Hoose, C. and Möhler, O.: Heterogeneous ice nucleation on atmospheric aerosols: A review of results from laboratory experiments, 9817-9854 pp., https://doi.org/10.5194/acp-12-9817-2012, 2012.

Hoose, C., Lohmann, U., Erdin, R., and Tegen, I.: The global influence of dust mineralogical composition on heterogeneous ice nucleation in mixed-phase clouds, Environ. Res. Lett., 3, 025003, https://doi.org/10.1088/1748-9326/3/2/025003, 2008.

Hoose, C., Kristjánsson, J. E., and Burrows, S. M.: How important is biological ice nucleation in clouds on a global scale?, Environ. Res. Lett., 5, 024009, https://doi.org/10.1088/1748-9326/5/2/024009, 2010.

Huang, S., Hu, W., Chen, J., Wu, Z., Zhang, D., and Fu, P.: Overview of biological ice nucleating particles in the atmosphere, Environ. Int., 146, 106197, https://doi.org/10.1016/j.envint.2020.106197, 2021.

Huang, W. T. K., Ickes, L., Tegen, I., Rinaldi, M., Ceburnis, D., and Lohmann, U.: Global relevance of marine organic aerosol as ice nucleating particles, Atmos. Chem. Phys., 18, 11423–11445, https://doi.org/10.5194/acp-18-11423-2018, 2018.

Huffman, J. A., Prenni, A. J., DeMott, P. J., Pöhlker, C., Mason, R. H., Robinson, N. H., Fröhlich-Nowoisky, J., Tobo, Y., Després, V. R., Garcia, E., Gochis, D. J., Harris, E., Müller-Germann, I., Ruzene, C., Schmer, B., Sinha, B., Day, D. A., Andreae, M. O., Jimenez, J. L., Gallagher, M., Kreidenweis, S. M., Bertram, A. K., and Pöschl, U.: High concentrations of biological aerosol particles and ice nuclei during and after rain, Atmos. Chem. Phys., 13, 6151–6164, https://doi.org/10.5194/acp-13-6151-2013, 2013.

Hummel, M., Hoose, C., Gallagher, M., Healy, D. A., Huffman, J. A., O'Connor, D., Pöschl, U., Pöhlker, C., Robinson, N. H., Schnaiter, M., Sodeau, J. R., Stengel, M., Toprak, E., and Vogel, H.: Regional-scale simulations of fungal spore aerosols using an emission parameterization adapted to local measurements of fluorescent biological aerosol particles, Atmos. Chem. Phys., 15, 6127–6146, https://doi.org/10.5194/acp-15-6127-2015, 2015.

Jahl, L. G., Brubaker, T. A., Polen, M. J., Jahn, L. G., Cain, K. P., Bowers, B. B., Fahy, W. D., Graves, S., and Sullivan, R. C.: Atmospheric aging enhances the ice nucleation ability of biomass-burning aerosol, Sci. Adv., 7, 1–10, https://doi.org/10.1126/sciadv.abd3440, 2021.

Jeuken, M., Van Wijk, R., Peleman, J., and Lindhout, P.: An integrated interspecific AFLP map of lettuce (Lactuca) based on two L. sativa × L. saligna F2 populations, Theor. Appl. Genet., 103, 638–647, https://doi.org/10.1007/s001220100657, 2001.

~~Journet, E., Balkanski, Y., and Harrison, S. P.: A new data set of soil mineralogy for dust-cycle modeling, Atmos. Chem. Phys., 14, 3801–3816, https://doi.org/10.5194/acp-14-3801-2014, 2014.~~

Kalivitis, N., Gerasopoulos, E., Vrekoussis, M., Kouvarakis, G., Kubilay, N., Hatzianastassiou, N., Vardavas, I., and Mihalopoulos, N.: Dust transport over the eastern mediterranean derived from total ozone mapping spectrometer, aerosol robotic network, and surface measurements, J. Geophys. Res. Atmos., 112, https://doi.org/10.1029/2006JD007510, 2007.

Kanakidou, M., Duce, R. A., Prospero, J. M., Baker, A. R., Benitez-Nelson, C., Dentener, F. J., Hunter, K. A., Liss, P. S., Mahowald, N., Okin, G. S., Sarin, M., Tsigaridis, K., Uematsu, M., Zamora, L. M., and Zhu, T.: Atmospheric fluxes of organic N and P to the global ocean, Global Biogeochem. Cycles, 26, 1–12, https://doi.org/10.1029/2011GB004277, 2012.

Kanakidou, M., Myriokefalitakis, S., and Tsagkaraki, M.: Atmospheric inputs of nutrients to the Mediterranean Sea, Deep. Res. Part II Top. Stud. Oceanogr., 171, https://doi.org/10.1016/j.dsr2.2019.06.014, 2020.

Kanji, Z. A., Ladino, L. A., Wex, H., Boose, Y., Burkert-Kohn, M., Cziczo, D. J., and Krämer, M.: Overview of Ice Nucleating Particles, Meteorol. Monogr., 58, 1.1-1.33, https://doi.org/10.1175/AMSMONOGRAPHS-D-16-0006.1, 2017.

Kluska, K., Piotrowicz, K., and Kasprzyk, I.: The impact of rainfall on the diurnal patterns of atmospheric pollen concentrations, Agric. For. Meteorol., 291, 108042, https://doi.org/10.1016/j.agrformet.2020.108042, 2020.

Kok, J. F.: A scaling theory for the size distribution of emitted dust aerosols suggests climate models underestimate the size of the global dust cycle, Proc. Natl. Acad. Sci. U. S. A., 108, 1016–1021, https://doi.org/10.1073/pnas.1014798108, 2011.

Korolev, A.: Limitations of the Wegener–Bergeron–Findeisen Mechanism in the Evolution of Mixed-Phase Clouds, J. Atmos. Sci., 64, 3372–3375, https://doi.org/10.1175/JAS4035.1, 2007.

Korolev, A. and Leisner, T.: Review of experimental studies of secondary ice production, Atmos. Chem. Phys., 20, 11767–11797, https://doi.org/10.5194/acp-20-11767-2020, 2020.

Korolev, A. and Milbrandt, J.: How Are Mixed-Phase Clouds Mixed?, Geophys. Res. Lett., 49, 1–7, https://doi.org/10.1029/2022GL099578, 2022.

Kumar, A., Marcolli, C., and Peter, T.: Ice nucleation activity of silicates and aluminosilicates in pure water and aqueous solutions. Part 2 – Quartz and amorphous silica, Atmos. Chem. Phys. Discuss., 1–35, https://doi.org/10.5194/acp-2018-1020, 2019a.

Kumar, A., Marcolli, C., and Peter, T.: Ice nucleation activity of silicates and aluminosilicates in pure water and aqueous solutions – Part 3: Aluminosilicates, Atmos. Chem. Phys., 19, 6059–6084, https://doi.org/10.5194/acp-19-6059-2019, 2019b.

Kumar, A., Klumpp, K., Barak, C., Rytwo, G., Plötze, M., Peter, T., and Marcolli, C.: Ice nucleation by smectites: The role of the edges, Atmos. Chem. Phys., 23, 4881–4902, https://doi.org/10.5194/acp-23-4881-2023, 2023.

Lebel, T., Parker, D. J., Flamant, C., Bourlès, B., Marticorena, B., Mougin, E., Peugeot, C., Diedhiou, A., Haywood, J. M., Ngamini, J. B., Polcher, J., Redelsperger, J. L., and Thorncroft, C. D.: The AMMA field campaigns: Multiscale and multidisciplinary observations in the West African region, Q. J. R. Meteorol. Soc., 136, 8–33, https://doi.org/10.1002/qj.486, 2010.

Lee, H. J. (Julie), Laskin, A., Laskin, J., and Nizkorodov, S. A.: Excitation–Emission Spectra and Fluorescence Quantum Yields for Fresh and Aged Biogenic Secondary Organic Aerosols, Environ. Sci. Technol., 47, 5763–5770, https://doi.org/10.1021/es400644c, 2013.

Liu, D., Wang, Z., Liu, Z., Winker, D., and Trepte, C.: A height resolved global view of dust aerosols from the first year CALIPSO lidar measurements, J. Geophys. Res. Atmos., 113, 1–15, https://doi.org/10.1029/2007JD009776, 2008.

~~Liu, X., Shi, X., Zhang, K., Jensen, E. J., Gettelman, A., Barahona, D., Nenes, A., and Lawson, P.: Sensitivity studies of dust ice nuclei effect on cirrus clouds with the Community Atmosphere Model CAM5, Atmos. Chem. Phys., 12, 12061–12079, https://doi.org/10.5194/acp-12-12061-2012, 2012.~~

Losey, D. J., Sihvonen, S. K., Veghte, D. P., Chong, E., and Freedman, M. A.: Acidic processing of fly ash: chemical characterization, morphology, and immersion freezing, Environ. Sci. Process. Impacts, 20, 1581–1592, https://doi.org/10.1039/c8em00319j, 2018.

Louis, J.-F.: A parametric model of vertical eddy fluxes in the atmosphere, Boundary-Layer Meteorol., 17, 187–202, https://doi.org/10.1007/BF00117978, 1979.

Marticorena, B., Chatenet, B., Rajot, J. L., Traoré, S., Coulibaly, M., Diallo, A., Koné, I., Maman, A., Ndiaye, T., and Zakou, A.: Temporal variability of mineral dust concentrations over West Africa: Analyses of a pluriannual monitoring

from the AMMA Sahelian Dust Transect, Atmos. Chem. Phys., 10, 8899–8915, https://doi.org/10.5194/acp-10-8899-2010, 2010.

Mason, R. H., Si, M., Li, J., Chou, C., Dickie, R., Toom-Sauntry, D., Pöhlker, C., Yakobi-Hancock, J. D., Ladino, L. A., Jones, K., Leaitch, W. R., Schiller, C. L., Abbatt, J. P. D., Huffman, J. A., and Bertram, A. K.: Ice nucleating particles at a coastal marine boundary layer site: Correlations with aerosol type and meteorological conditions, Atmos. Chem. Phys., 15, 12547–12566, https://doi.org/10.5194/acp-15-12547-2015, 2015.

McCluskey, C. S., Hill, T. C. J., Malfatti, F., Sultana, C. M., Lee, C., Santander, M. V, Beall, C. M., Moore, K. A., Cornwell, G. C., Collins, D. B., Prather, K. A., Jayarathne, T., Stone, E. A., Azam, F., Kreidenweis, S. M., and DeMott, P. J.: A Dynamic Link between Ice Nucleating Particles Released in Nascent Sea Spray Aerosol and Oceanic Biological Activity during Two Mesocosm Experiments, J. Atmos. Sci., 74, 151–166, https://doi.org/10.1175/JAS-D-16-0087.1, 2017.

McCluskey, C. S., Ovadnevaite, J., Rinaldi, M., Atkinson, J., Belosi, F., Ceburnis, D., Marullo, S., Hill, T. C. J., Lohmann, U., Kanji, Z. A., O'Dowd, C., Kreidenweis, S. M., and DeMott, P. J.: Marine and Terrestrial Organic Ice-Nucleating Particles in Pristine Marine to Continentally Influenced Northeast Atlantic Air Masses, J. Geophys. Res. Atmos., 123, 6196–6212, https://doi.org/10.1029/2017JD028033, 2018.

Mitts, B.McCluskey, C. S., Gettelman, A., Wang, X., Lucero, D. D., Beall, C. M., Deane,Bardeen, C. G. B., DeMott, P. J., and PratherMoore, K. A.: Importance of Supermicron., Kreidenweis, S. M., Hill, T. C. J., Barry, K. R., Twohy, C. H., Toohey, D. W., Rainwater, B., Jensen, J. B., Reeves, J. M., Alexander, S. P., and McFarquhar, G. M.: Simulating Southern Ocean Aerosol and Ice Nucleating Particles in Nascent Sea Spray,the Community Earth System Model Version 2, J. Geophys. Res. Lett., 48, e2020GL089633Atmos., 128, 1–21, https://doi.org/https://doi.org/10.1029/2020GL089633, 20212022JD036955, 2023.

Morrison, D., Crawford, I., Marsden, N., Flynn, M., Read, K., Neves, L., Foot, V., Kaye, P., Stanley, W., Coe, H., Topping, D., and Gallagher, M.: Quantifying bioaerosol concentrations in dust clouds through online UV-LIF and mass spectrometry measurements at the Cape Verde Atmospheric Observatory, Atmos. Chem. Phys., 20, 14473–14490, https://doi.org/10.5194/acp-20-14473-2020, 2020.

Murray, B. J., O'Sullivan, D., Atkinson, J. D., and Webb, M. E.: Ice nucleation by particles immersed in supercooled cloud droplets, Chem. Soc. Rev., 41, 6519, https://doi.org/10.1039/c2cs35200a, 2012.

Murray, B. J., Carslaw, K. S., and Field, P. R.: Opinion: Cloud-phase climate feedback and the importance of ice-nucleating particles, Atmos. Chem. Phys., 21, 665–679, https://doi.org/10.5194/acp-21-665-2021, 2021.

Myriokefalitakis, S., Vignati, E., Tsigaridis, K., Papadimas, C., Sciare, J., Mihalopoulos, N., Facchini, M. C., Rinaldi, M., Dentener, F. J., Ceburnis, D., Hatzianastasiou, N., O'Dowd, C. D., van Weele, M., and Kanakidou, M.: Global Modeling of the Oceanic Source of Organic Aerosols, Adv. Meteorol., 2010, 1–16, https://doi.org/10.1155/2010/939171, 2010.

Myriokefalitakis, S., Daskalakis, N., Mihalopoulos, N., Baker, A. R., Nenes, A., and Kanakidou, M.: Changes in dissolved iron deposition to the oceans driven by human activity: a 3-D global modelling study, Biogeosciences, 12, 3973–3992, https://doi.org/10.5194/bg-12-3973-2015, 2015.

Myriokefalitakis, S., Nenes, A., Baker, A. R., Mihalopoulos, N., and Kanakidou, M.: Bioavailable atmospheric phosphorous supply to the global ocean: a 3-D global modelling study, Biogeosciences Discuss., 0, 1–28, https://doi.org/10.5194/bg-2016-215, 2016.

Myriokefalitakis, S., Fanourgakis, G., and Kanakidou, M.: The Contribution of Bioaerosols to the Organic Carbon Budget of the Atmosphere, in: Perspectives on Atmospheric Sciences, edited by: Karacostas, T., Bais, A., and Nastos, P. T.,

Springer International Publishing, Cham, 845–851, https://doi.org/10.1007/978-3-319-35095-0_121, 2017.

Naud, C. M., Booth, J. F., and Genio, A. D. Del: Evaluation of ERA-Interim and MERRA Cloudiness in the Southern Ocean, J. Clim., 27, 2109–2124, https://doi.org/10.1175/JCLI-D-13-00432.1, 2014.

Negron, A., DeLeon-Rodriguez, N., Waters, S. M., Ziemba, L. D., Anderson, B., Bergin, M., Konstantinidis, K. T., and Nenes, A.: Using flow cytometry and light-induced fluorescence to characterize the variability and characteristics of bioaerosols in springtime in Metro Atlanta, Georgia, Atmos. Chem. Phys., 20, 1817–1838, https://doi.org/10.5194/acp-20-1817-2020, 2020.

Nickovic, S., Vukovic, A., Vujadinovic, M., Djurdjevic, V., and Pejanovic, G.: Technical Note: High-resolution mineralogical database of dust-productive soils for atmospheric dust modeling, Atmos. Chem. Phys., 12, 845–855, https://doi.org/10.5194/acp-12-845-2012, 2012.

Van Noije, T. P. C., Le Sager, P., Segers, A. J., Van Velthoven, P. F. J., Krol, M. C., Hazeleger, W., Williams, A. G., and Chambers, S. D.: Simulation of tropospheric chemistry and aerosols with the climate model EC-Earth, Geosci. Model Dev., 7, 2435–2475, https://doi.org/10.5194/gmd-7-2435-2014, 2014.

O'Dowd, C. D., ~~Facchini, M. C., Cavalli, F., Ceburnis, D., Mircea, M., Decesari, S., Fuzzi, S., Young, J. Y., and Putaud, J. P.: Biogenically driven organic contribution to marine aerosol, Nature, 431, 676–680, https://doi.org/10.1038/nature02959, 2004.~~

~~O'Dowd, C. D.,~~ Langmann, B., Varghese, S., Scannell, C., Ceburnis, D., and Facchini, M. C.: A combined organic-inorganic sea-spray source function, Geophys. Res. Lett., 35, L01801, https://doi.org/10.1029/2007GL030331, 2008.

O'Sullivan, D., Murray, B. J., Ross, J. F., and Webb, M. E.: The adsorption of fungal ice-nucleating proteins on mineral dusts: a terrestrial reservoir of atmospheric ice-nucleating particles, Atmos. Chem. Phys., 16, 7879–7887, https://doi.org/10.5194/acp-16-7879-2016, 2016.

Olivié, D. J. L., van Velthoven, P. F. J., Beljaars, A. C. M., and Kelder, H. M.: Comparison between archived and off-line diagnosed convective mass fluxes in the chemistry transport model TM3, J. Geophys. Res. Atmos., 109, 1–13, https://doi.org/10.1029/2003JD004036, 2004.

Olson, J.: Major World Ecosystem Complexes Ranked by Carbon in Live Vegetation: A Database (NDP-017) (2001 version of original 1985 data). Carbon Dioxide Information Analysis Center (CDIAC), Oak Ridge National Laboratory (ORNL), Oak Ridge, TN (United States), ESS-DI, https://doi.org/10.3334/CDIAC/LUE.NDP017, 1992.

Paytan, A., Cade-Menun, B. J., McLaughlin, K., and Faul, K. L.: Selective phosphorus regeneration of sinking marine particles: evidence from 31P-NMR, Mar. Chem., 82, 55–70, https://doi.org/10.1016/S0304-4203(03)00052-5, 2003.

Peckhaus, A., Kiselev, A., Hiron, T., Ebert, M., and Leisner, T.: A comparative study of K-rich and Na/Ca-rich feldspar ice-nucleating particles in a nanoliter droplet freezing assay, Atmos. Chem. Phys., 16, 11477–11496, https://doi.org/10.5194/acp-16-11477-2016, 2016.

Perlwitz, J. P., Pérez García-Pando, C., and Miller, R. L.: Predicting the mineral composition of dust aerosols – Part 1: Representing key processes, Atmos. Chem. Phys., 15, 11593–11627, https://doi.org/10.5194/acp-15-11593-2015, 2015a.

Perlwitz, J. P., Pérez García-Pando, C., and Miller, R. L.: Predicting the mineral composition of dust aerosols – Part 2: Model evaluation and identification of key processes with observations, Atmos. Chem. Phys., 15, 11629–11652, https://doi.org/10.5194/acp-15-11629-2015, 2015b.

Pikridas, M., Vrekoussis, M., Sciare, J., Kleanthous, S., Vasiliadou, E., Kizas, C., Savvides, C., and Mihalopoulos, N.: Spatial and temporal (short and long-term) variability of submicron, fine and sub-10 Mm particulate matter (PM1, PM2.5, PM10) in Cyprus, Atmos. Environ., 191, 79–93, https://doi.org/10.1016/j.atmosenv.2018.07.048, 2018.

Pöschl, U., Martin, S. T., Sinha, B., Chen, Q., Gunthe, S. S., Huffman, J. A., Borrmann, S., Farmer, D. K., Garland, R.

M., Helas, G., Jimenez, J. L., King, S. M., Manzi, A., Mikhailov, E., Pauliquevis, T., Petters, M. D., Prenni, A. J., Roldin, P., Rose, D., Schneider, J., Su, H., Zorn, S. R., Artaxo, P., and Andreae, M. O.: Rainforest Aerosols as Biogenic Nuclei of Clouds and Precipitation in the Amazon, Science (80-.)., 329, 1513–1516, https://doi.org/10.1126/science.1191056, 2010.

Prenni, A. J., Petters, M. D., Kreidenweis, S. M., Heald, C. L., Martin, S. T., Artaxo, P., Garland, R. M., Wollny, A. G., and Pöschl, U.: Relative roles of biogenic emissions and Saharan dust as ice nuclei in the Amazon basin, Nat. Geosci., 2, 402–405, https://doi.org/10.1038/ngeo517, 2009.

Prospero, J. M.: Long-term measurements of the transport of African mineral dust to the southeastern United States: Implications for regional air quality, J. Geophys. Res. Atmos., 104, 15917–15927, https://doi.org/10.1029/1999JD900072, 1999.

Prospero, J. M., Barkley, A. E., Gaston, C. J., Gatineau, A., Campos y Sansano, A., and Panechou, K.: Characterizing and Quantifying African Dust Transport and Deposition to South America: Implications for the Phosphorus Budget in the Amazon Basin, Global Biogeochem. Cycles, 34, 1–24, https://doi.org/10.1029/2020GB006536, 2020.

Pruppacher, H. R., Klett, J. D., and Wang, P. K.: Microphysics of Clouds and Precipitation, Aerosol Sci. Technol., 28, 381–382, https://doi.org/10.1080/02786829808965531, 1998.

Pummer, B. G., Bauer, H., Bernardi, J., Bleicher, S., and Grothe, H.: Suspendable macromolecules are responsible for ice nucleation activity of birch and conifer pollen, Atmos. Chem. Phys., 12, 2541–2550, https://doi.org/10.5194/acp-12-2541-2012, 2012.

Pummer, B. G., Budke, C., Augustin-Bauditz, S., Niedermeier, D., Felgitsch, L., Kampf, C. J., Huber, R. G., Liedl, K. R., Loerting, T., Moschen, T., Schauperl, M., Tollinger, M., Morris, C. E., Wex, H., Grothe, H., Pöschl, U., Koop, T., and Fröhlich-Nowoisky, J.: Ice nucleation by water-soluble macromolecules, Atmos. Chem. Phys., 15, 4077–4091, https://doi.org/10.5194/acp-15-4077-2015, 2015.

Raman, A., Hill, T., Demott, P. J., Singh, B., Zhang, K., Ma, P. L., Wu, M., Wang, H., Alexander, S. P., and Burrows, S. M.: Long-term variability in immersion-mode marine ice-nucleating particles from climate model simulations and observations, Atmos. Chem. Phys., 23, 5735–5762, https://doi.org/10.5194/acp-23-5735-2023, 2023.

Ramelli, F., Henneberger, J., David, R. O., Bühl, J., Radenz, M., Seifert, P., Wieder, J., Lauber, A., Pasquier, J. T., Engelmann, R., Mignani, C., Hervo, M., and Lohmann, U.: Microphysical investigation of the seeder and feeder region of an Alpine mixed-phase cloud, Atmos. Chem. Phys., 21, 6681–6706, https://doi.org/10.5194/acp-21-6681-2021, 2021.

Rinaldi, M., Decesari, S., Finessi, E., Giulianelli, L., Carbone, C., Fuzzi, S., O'Dowd, C. D., Ceburnis, D., and Facchini, M. C.: Primary and Secondary Organic Marine Aerosol and Oceanic Biological Activity: Recent Results and New Perspectives for Future Studies, Adv. Meteorol., 2010, https://doi.org/10.1155/2010/310682, 2010

Russell, G. L. and Lerner, J. A.: A New Finite-Differencing Scheme for the Tracer Transport Equation, J. Appl. Meteorol., 20, 1483–1498, https://doi.org/10.1175/1520-0450(1981)020<1483:ANFDSF>2.0.CO;2, 1981.

Sassen, K., DeMott, P. J., Prospero, J. M., and Poellot, M. R.: Saharan dust storms and indirect aerosol effects on clouds: CRYSTAL-FACE results, Geophys. Res. Lett., 30, 1–4, https://doi.org/10.1029/2003GL017371, 2003.

Sciare, J., Favez, O., Sarda-Estève, R., Oikonomou, K., Cachier, H., and Kazan, V.: Long-term observations of carbonaceous aerosols in the Austral Ocean atmosphere: Evidence of a biogenic marine organic source, J. Geophys. Res. Atmos., 114, 1–10, https://doi.org/10.1029/2009JD011998, 2009.

Seinfeld, J. H. and Pandis, S. N.: Atmospheric chemistry and physics : from air pollution to climate change, New York (N.Y.) : Wiley, 1998.

Shaw, R. A., Durant, A. J., and Mi, Y.: Heterogeneous Surface Crystallization Observed in Undercooled Water, J. Phys.

Chem. B, 109, 9865–9868, https://doi.org/10.1021/jp0506336, 2005.

Si, M., Evoy, E., Yun, J., Xi, Y., Hanna, S. J., Chivulescu, A., Rawlings, K., Veber, D., Platt, A., Kunkel, D., Hoor, P., Sharma, S., Richard Leaitch, W., and Bertram, A. K.: Concentrations, composition, and sources of ice-nucleating particles in the Canadian High Arctic during spring 2016, Atmos. Chem. Phys., 19, 3007–3024, https://doi.org/10.5194/acp-19-3007-2019, 2019.

Sorooshian, A., Feingold, G., Lebsock, M. D., Jiang, H., and Stephens, G. L.: On the precipitation susceptibility of clouds to aerosol perturbations, Geophys. Res. Lett., 36, L13803, https://doi.org/10.1029/2009GL038993, 2009.

Spracklen, D. V. and Heald, C. L.: The contribution of fungal spores and bacteria to regional and global aerosol number and ice nucleation immersion freezing rates, Atmos. Chem. Phys., 14, 9051–9059, https://doi.org/10.5194/acp-14-9051-2014, 2014.

Subba, T., Zhang, Y., and Steiner, A. L.: Simulating the Transport and Rupture of Pollen in the Atmosphere, J. Adv. Model. Earth Syst., 15, 1–25, https://doi.org/10.1029/2022MS003329, 2023.

Sullivan, S. C., Hoose, C., Kiselev, A., Leisner, T., and Nenes, A.: Initiation of secondary ice production in clouds, Atmos. Chem. Phys., 18, 1593–1610, https://doi.org/10.5194/acp-18-1593-2018, 2018.

Suski, K. J., Hill, T. C. J., Levin, E. J. T., Miller, A., DeMott, P. J., and Kreidenweis, S. M.: Agricultural harvesting emissions of ice-nucleating particles, Atmos. Chem. Phys., 18, 13755–13771, https://doi.org/10.5194/acp-18-13755-2018, 2018.

Tegen, I., Harrison, S. P., Kohfeld, K., Prentice, I. C., Coe, M., and Heimann, M.: Impact of vegetation and preferential source areas on global dust aerosol: Results from a model study, J. Geophys. Res. Atmos., 107, https://doi.org/10.1029/2001JD000963, 2002.

Tiedtke, M.: A Comprehensive Mass Flux Scheme for Cumulus Parameterization in Large-Scale Models, Mon. Weather Rev., 117, 1779–1800, https://doi.org/10.1175/1520-0493(1989)117<1779:ACMFSF>2.0.CO;2, 1989.

Tobo, Y., Prenni, A. J., Demott, P. J., Huffman, J. A., McCluskey, C. S., Tian, G., Pöhlker, C., Pöschl, U., and Kreidenweis, S. M.: Biological aerosol particles as a key determinant of ice nuclei populations in a forest ecosystem, J. Geophys. Res. Atmos., 118, 10,100-10,110, https://doi.org/10.1002/jgrd.50801, 2013.

Tsigaridis, K. and Kanakidou, M.: Global modelling of secondary organic aerosol in the troposphere: a sensitivity analysis, Atmos. Chem. Phys., 3, 1849–1869, https://doi.org/10.5194/acp-3-1849-2003, 2003.

Tsigaridis, K. and Kanakidou, M.: Secondary organic aerosol importance in the future atmosphere, Atmos. Environ., 41, 4682–4692, https://doi.org/10.1016/j.atmosenv.2007.03.045, 2007.

Tsigaridis, K., Krol, M., Dentener, F. J., Balkanski, Y., Lathière, J., Metzger, S., Hauglustaine, D. A., and Kanakidou, M.: Change in global aerosol composition since preindustrial times, Atmos. Chem. Phys., 6, 5143–5162, https://doi.org/10.5194/acp-6-5143-2006, 2006.

Vali, G., DeMott, P. J., Möhler, O., and Whale, T. F.: Technical Note: A proposal for ice nucleation terminology, Atmos. Chem. Phys., 15, 10263–10270, https://doi.org/10.5194/acp-15-10263-2015, 2015.

Vergara-Temprado, J., Murray, B. J., Wilson, T. W., O'Sullivan, D., Browse, J., Pringle, K. J., Ardon-Dryer, K., Bertram, A. K., Burrows, S. M., Ceburnis, D., DeMott, P. J., Mason, R. H., O'Dowd, C. D., Rinaldi, M., and Carslaw, K. S.: Contribution of feldspar and marine organic aerosols to global ice nucleating particle concentrations, Atmos. Chem. Phys., 17, 3637–3658, https://doi.org/10.5194/acp-17-3637-2017, 2017.

Vergara-Temprado, J., Miltenberger, A. K., Furtado, K., Grosvenor, D. P., Shipway, B. J., Hill, A. A., Wilkinson, J. M., Field, P. R., Murray, B. J., and Carslaw, K. S.: Strong control of Southern Ocean cloud reflectivity by ice-nucleating particles, Proc. Natl. Acad. Sci. U. S. A., 115, 2687–2692, https://doi.org/10.1073/pnas.1721627115, 2018.

Vignati, E., Facchini, M. C., Rinaldi, M., Scannell, C., Ceburnis, D., Sciare, J., Kanakidou, M., Myriokefalitakis, S., Dentener, F., and O'Dowd, C. D.: Global scale emission and distribution of sea-spray aerosol: Sea-salt and organic enrichment, Atmos. Environ., 44, 670–677, https://doi.org/10.1016/j.atmosenv.2009.11.013, 2010.

~~Wang, X., Deane, G. B., Moore, K. A., Ryder, O. S., Stokes, M. D., Beall, C. M., Collins, D. B., Santander, M. V., Burrows, S. M., Sultana, C. M., and Prather, K. A.: The role of jet and film drops in controlling the mixing state of submicron sea spray aerosol particles., Proc. Natl. Acad. Sci. U. S. A., 114, 6978–6983, https://doi.org/10.1073/pnas.1702420114, 2017.~~

Welti, A., Bigg, E. K., Demott, P. J., Gong, X., Hartmann, M., Harvey, M., Henning, S., Herenz, P., Hill, T. C. J., Hornblow, B., Leck, C., Löffler, M., Mccluskey, C. S., Rauker, A. M., Schmale, J., Tatzelt, C., and Pinxteren, M. Van: Ship-based measurements of ice nuclei concentrations over the Arctic , Atlantic , Pacific and Southern oceans, 15191–15206, 2020.

Wex, H., Demott, P. J., Tobo, Y., Hartmann, S., Rösch, M., Clauss, T., Tomsche, L., Niedermeier, D., and Stratmann, F.: Kaolinite particles as ice nuclei: Learning from the use of different kaolinite samples and different coatings, Atmos. Chem. Phys., 14, 5529–5546, https://doi.org/10.5194/acp-14-5529-2014, 2014.

Whale, T. F., Holden, M. A., Wilson, T. W., O'Sullivan, D., and Murray, B. J.: The enhancement and suppression of immersion mode heterogeneous ice-nucleation by solutes, Chem. Sci., 9, 4142–4151, https://doi.org/10.1039/c7sc05421a, 2018.

Wieder, J., Ihn, N., Mignani, C., Haarig, M., Bühl, J., Seifert, P., Engelmann, R., Ramelli, F., Kanji, Z. A., Lohmann, U., and Henneberger, J.: Retrieving ice-nucleating particle concentration and ice multiplication factors using active remote sensing validated by in situ observations, Atmos. Chem. Phys., 22, 9767–9797, https://doi.org/10.5194/acp-22-9767-2022, 2022.

Wilson, T. W., Ladino, L. A., Alpert, P. A., Breckels, M. N., Brooks, I. M., Browse, J., Burrows, S. M., Carslaw, K. S., Huffman, J. A., Judd, C., Kilthau, W. P., Mason, R. H., McFiggans, G., Miller, L. A., Nájera, J. J., Polishchuk, E., Rae, S., Schiller, C. L., Si, M., Temprado, J. V., Whale, T. F., Wong, J. P. S., Wurl, O., Yakobi-Hancock, J. D., Abbatt, J. P. D., Aller, J. Y., Bertram, A. K., Knopf, D. A., and Murray, B. J.: A marine biogenic source of atmospheric ice-nucleating particles., Nature, 525, 234–8, https://doi.org/10.1038/nature14986, 2015.

Yi, B.: Diverse cloud radiative effects and global surface temperature simulations induced by different ice cloud optical property parameterizations, Sci. Rep., 12, 1–11, https://doi.org/10.1038/s41598-022-14608-w, 2022.

Yin, J., Wang, D., and Guoqing, Z.: An Evaluation of Ice Nuclei Characteristics from the Long-term Measurement Data over North China An Evaluation of Ice Nuclei Characteristics from the Long-term Measurement Data over North China, https://doi.org/10.1007/s13143-012-0020-8, 2012.

Zhang, D., Wang, Z., Heymsfield, A., Fan, J., Liu, D., and Zhao, M.: Quantifying the impact of dust on heterogeneous ice generation in midlevel supercooled stratiform clouds, Geophys. Res. Lett., 39, 1–6, https://doi.org/10.1029/2012GL052831, 2012.

Zhang, H., Zhao, M., Chen, Q., Wang, Q., Zhao, S., Zhou, X., and Peng, J.: Water and ice cloud optical thickness changes and radiative effects in East Asia, J. Quant. Spectrosc. Radiat. Transf., 254, 107213, https://doi.org/10.1016/j.jqsrt.2020.107213, 2020.

Zhao, X., Liu, X., Burrows, S. M., and Shi, Y.: Effects of marine organic aerosols as sources of immersion-mode ice-nucleating particles on high-latitude mixed-phase clouds, Atmos. Chem. Phys., 21, 2305–2327, https://doi.org/10.5194/acp-21-2305-2021, 2021.

Zhou, C., Zelinka, M. D., and Klein, S. A.: Impact of decadal cloud variations on the Earth's energy budget, Nat. Geosci.,

9, 871–874, https://doi.org/10.1038/ngeo2828, 2016.

Zolles, T., Burkart, J., Häusler, T., Pummer, B., Hitzenberger, R., and Grothe, H.: Identification of ice nucleation active sites on feldspar dust particles, J. Phys. Chem. A, 119, 2692–2700, https://doi.org/10.1021/jp509839x, 2015.

Zuidema, P., Alvarez, C., Kramer, S. J., Custals, L., Izaguirre, M., Sealy, P., Prospero, J. M., and Blades, E.: Is summer African dust arriving earlier to Barbados?, Bull. Am. Meteorol. Soc., 100, 1981–1986, https://doi.org/10.1175/BAMS-D-18-0083.1, 2019.

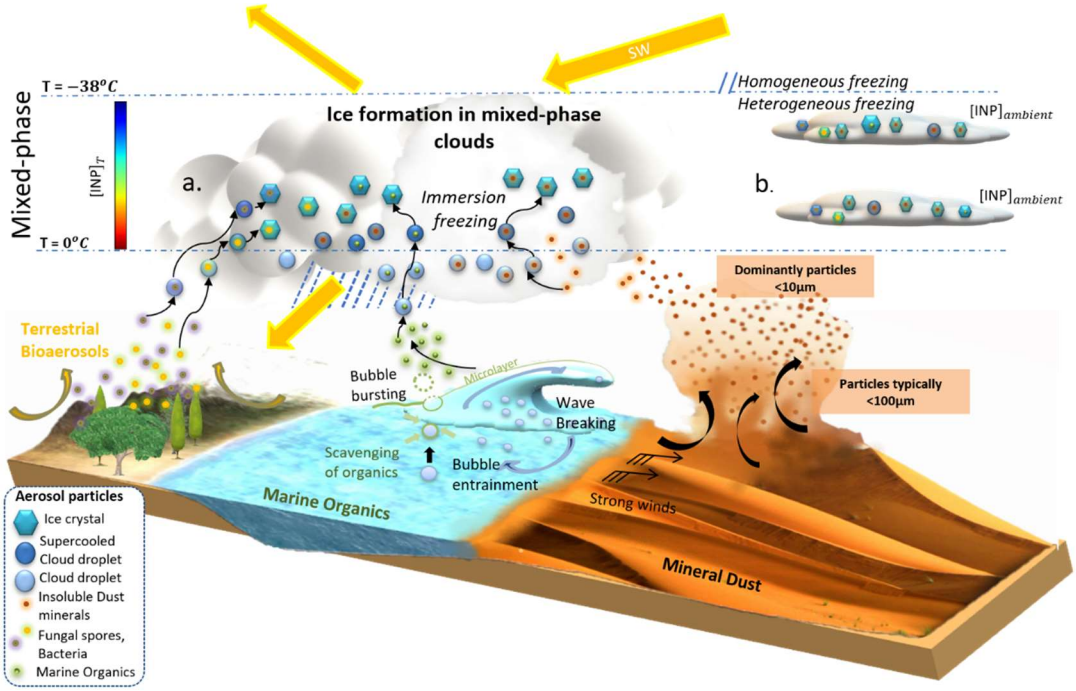

Figure 1: Illustration of the formation of INP from mineral dust, MPOA and PBAP, as well as the two ways in which we display INP concentrations in the present study: $[INP]_{ambient}$ is calculated at ambient model temperature relevant to non-deep convective mixed-phase clouds using the ambient temperature in the model temperature level (b.), and $[INP]_T$ is calculated at a fixed temperature relevant for vertically extended clouds as deep-convective systems (a.). The figure is based on Chatziparaschos et al. (2023).

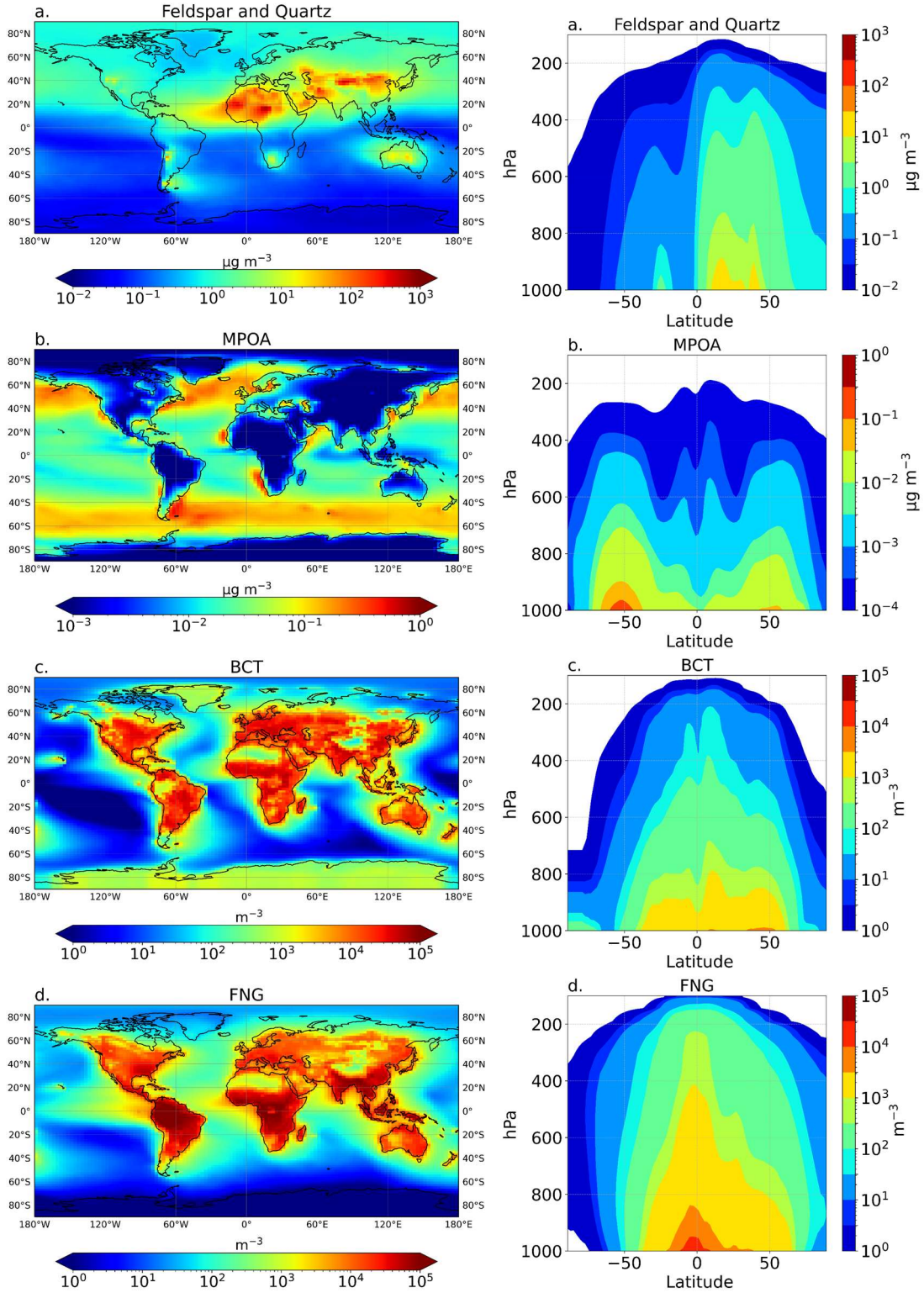

Figure 2: Simulated multi-year surface mean (left column) and zonal mean (right column) of (a) mineral dust (sum of K-feldspar and quartz) mass concentrations (μg m^{-3}), (b) primary marine organic aerosol mass concentrations (μg m^{-3}), (c) bacteria number concentrations (m^{-3}), (d) fungal spore number concentrations (m^{-3}).

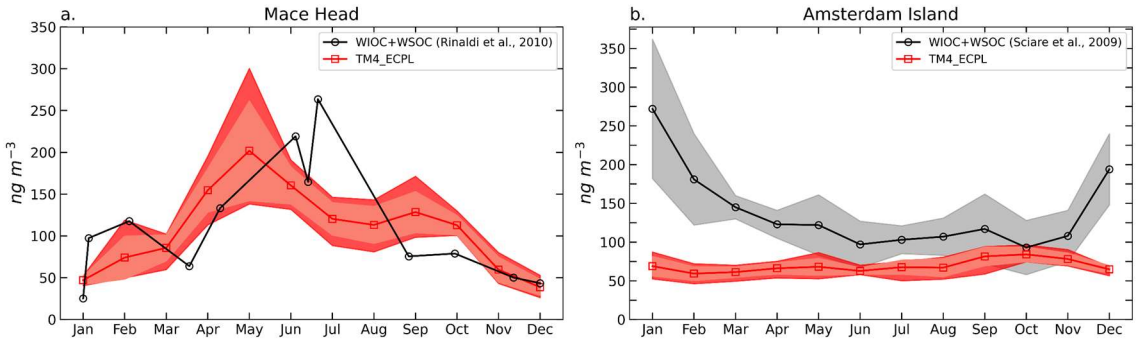

Figure 3: Monthly averaged concentrations of MPOA in ng-C m^{-3} at (a) Mace Head, (b) Amsterdam Island in ng-C m^{-3}. Observations from Rinaldi et al. (2010) and Sciare et al. (2009), respectively.

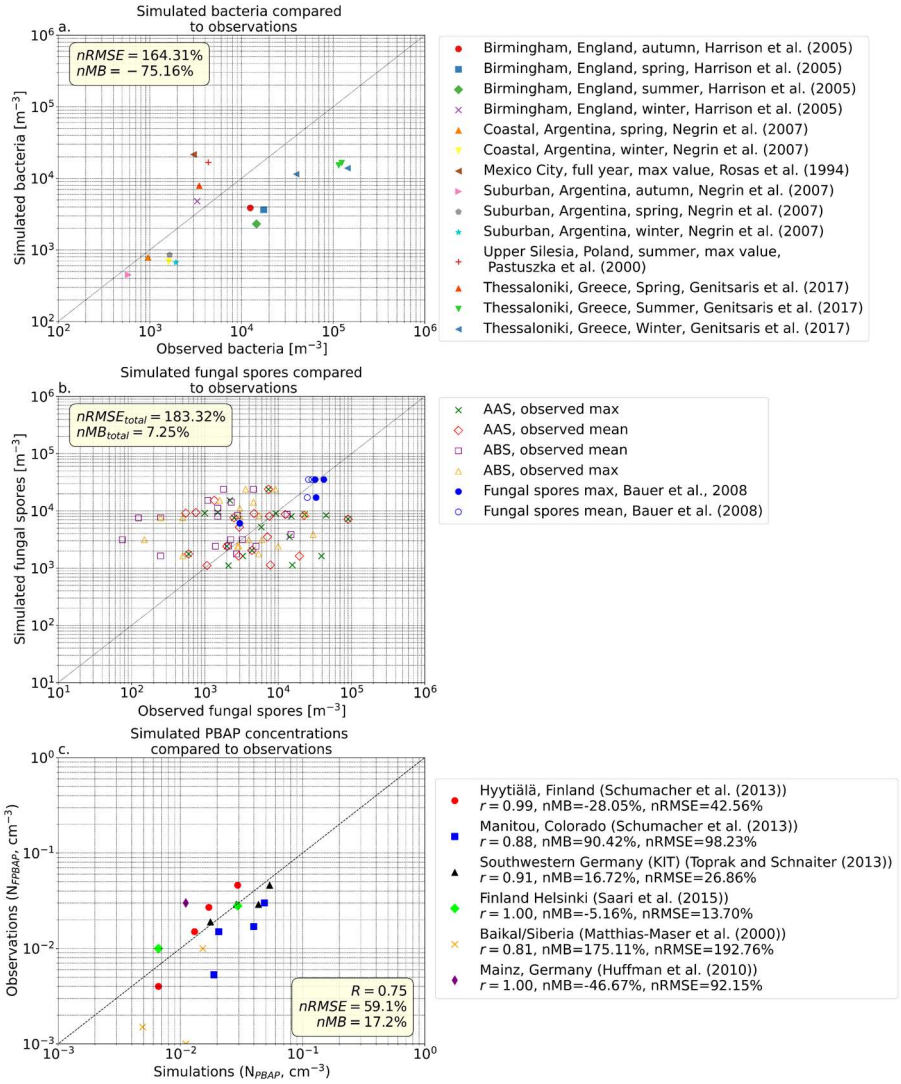

Figure 4: Simulated bioaerosol concentrations compared to observations. The observations are averages over different time periods, and the simulated data are taken for the corresponding months at the grid boxes containing the measurement site. (a). Bacteria concentrations; observations include concentrations listed in the supplement of Burrows et al. (2009) and Genitsaris et al. (2017). (b) Fungal spore concentrations, actively wet discharged ascospores (AAS) and basidiospores (ABS) compared to the simulated FNG. In the model, AAS and ABS are assumed to contribute one-third each to total

fungal spores. The observations are from the references listed in Elbert et al (2007) and Bauer et al. (2008). (c) Observations of fluorescent PBAP (FBAP) compared with model simulations of PBAP (for this comparison calculated as the sum of BCT, FNG and pollen). Observations are from the compilation of long-term measurements of atmospheric fluorescent bioaerosol number concentrations listed in Petersson Sjögren et al. (2023).

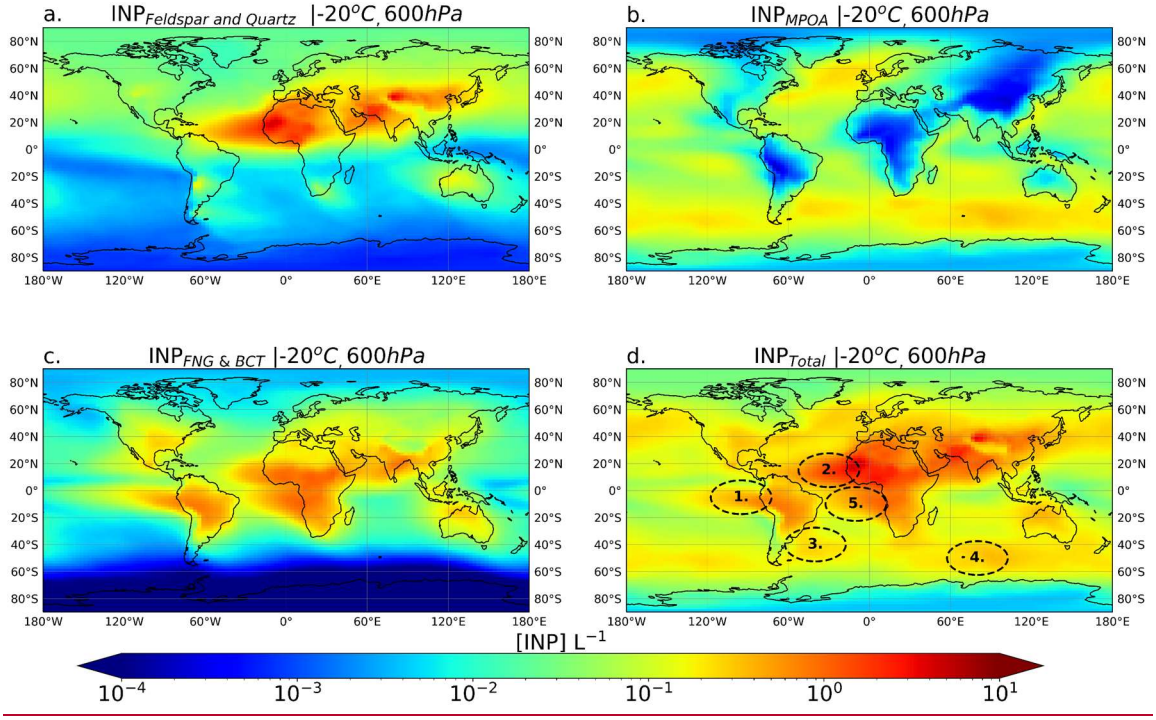

Figure 5: Multi-year mean distributions calculated by TM4-ECPL for INP number concentrations derived from dust (a), MPOA (b), PBAP (c), and the sum of the aforementioned INP (d) at a pressure level of 600 hPa for an activation temperature of −20°C. Circles labelled 1 to 5 indicate areas of interest, with numbering details provided in the main text.

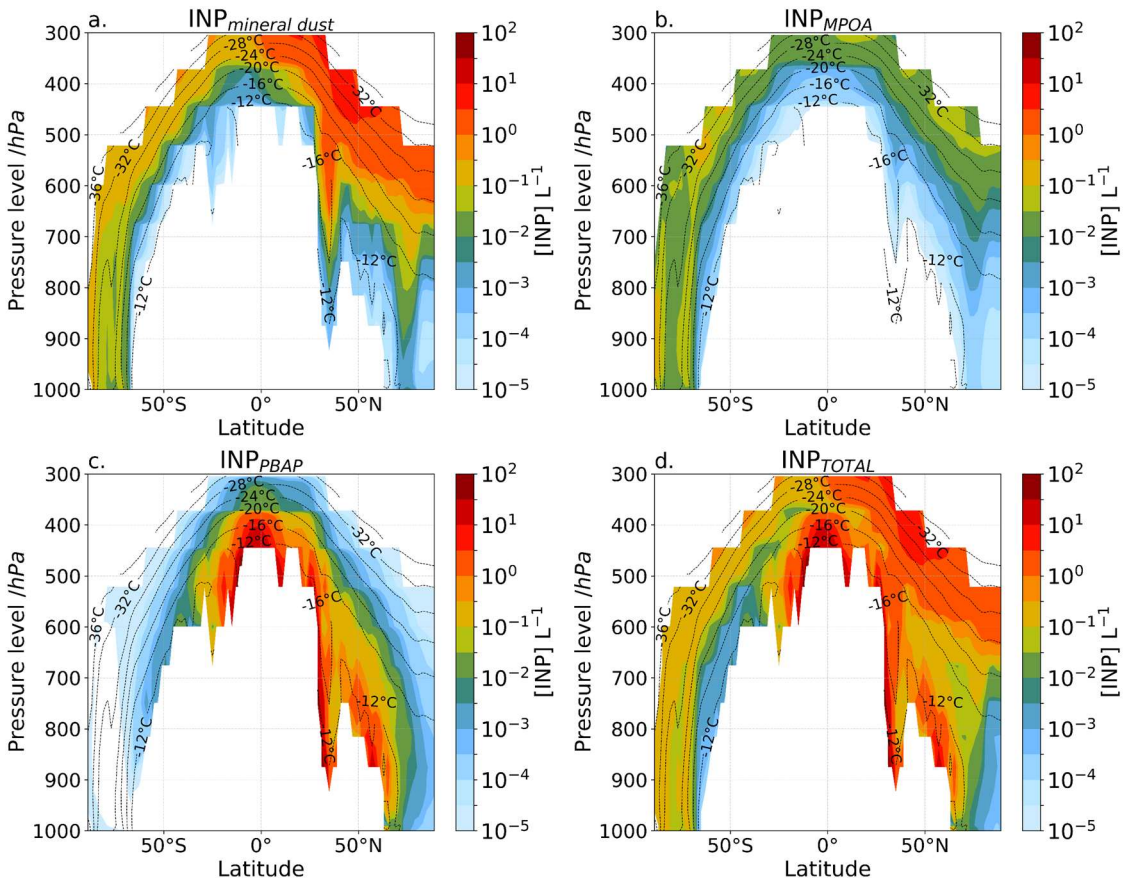

Figure 6: Multi-annual averaged zonal mean profiles of [INP] number concentration calculated at modelled ambient temperature by TM4-ECPL and accounting for (a) mineral dust, (b) marine bioaerosols, (c) fungal spores and bacteria (PBAP) and (d)all INP types in the model. The black contour dashed lines show the annual mean temperature of the model. The colours show (a-c) the INP number concentration.

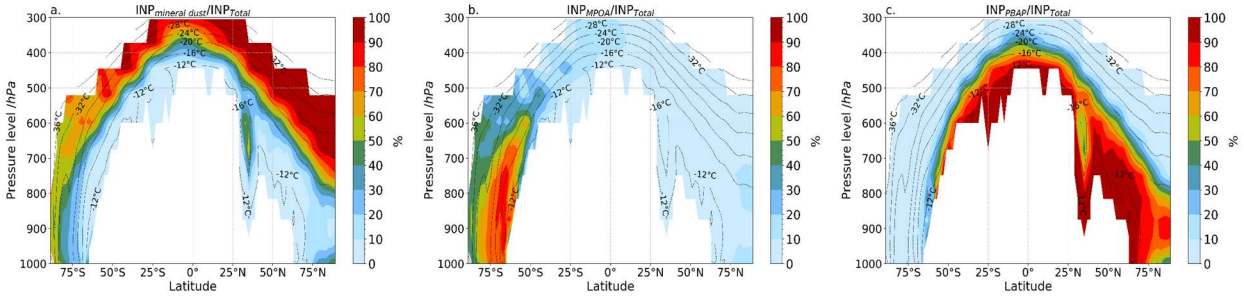

Figure 7: Multi-annual averaged zonal mean profiles of the percentage contribution of each species to the total INP number concentration, calculated at modelled ambient temperature by TM4-ECPL, showing contributions from (a) mineral dust, (b) marine bioaerosols and (c) fungal spores and bacteria (PBAP). Black dashed contour lines represent the model's annual mean temperature.

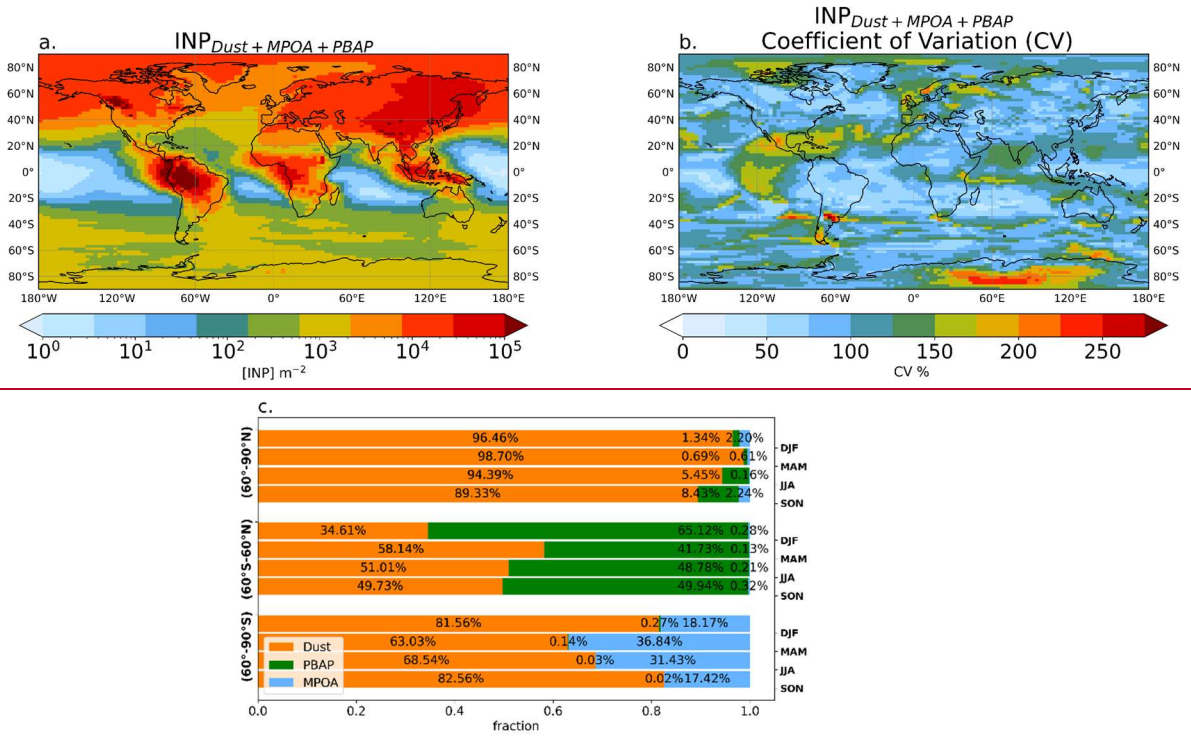

Figure 8: (a) Annual mean INP column number concentrations up to 300 hPa, for INP at modelled ambient temperature,(b) the interannual variability expressed by the coefficient of variation that is calculated as the standard deviation of the annual mean columns to the multiyear annual mean and is expressed in percent and (c) seasonal percentage contributions of INP from mineral dust (orange), MPOA (light blue), and PBAP (green), with data separated by middle latitudes (60°S–60°N) and high latitudes (60°–90°N, 60°–90°S).

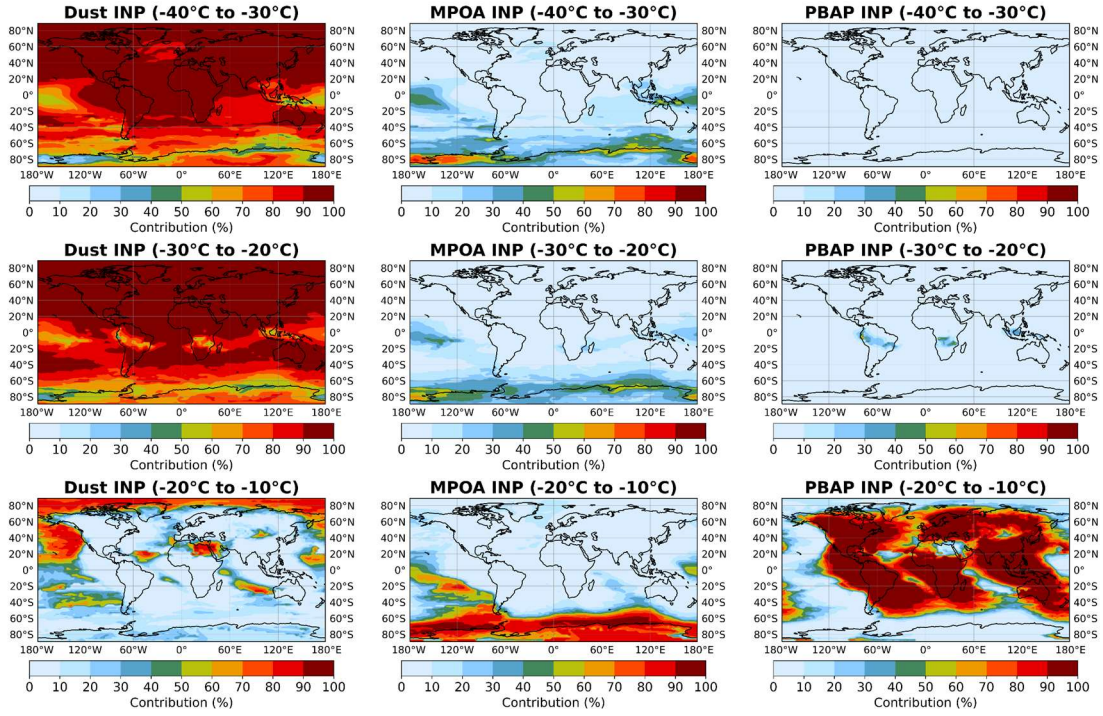

Figure 9: Multi-annual averaged percentage contributions of INP sources to the total INP column (surface up to 300 hPa): INP from mineral dust (left column), INP from MPOA (middle column), and INP from PBAP (right column), categorized by modelled temperature ranges: (top row) -40°C to -30°C, (middle row) -30°C to -20°C, and (bottom row) -20°C to -10°C. INP are calculated at modelled ambient temperature.

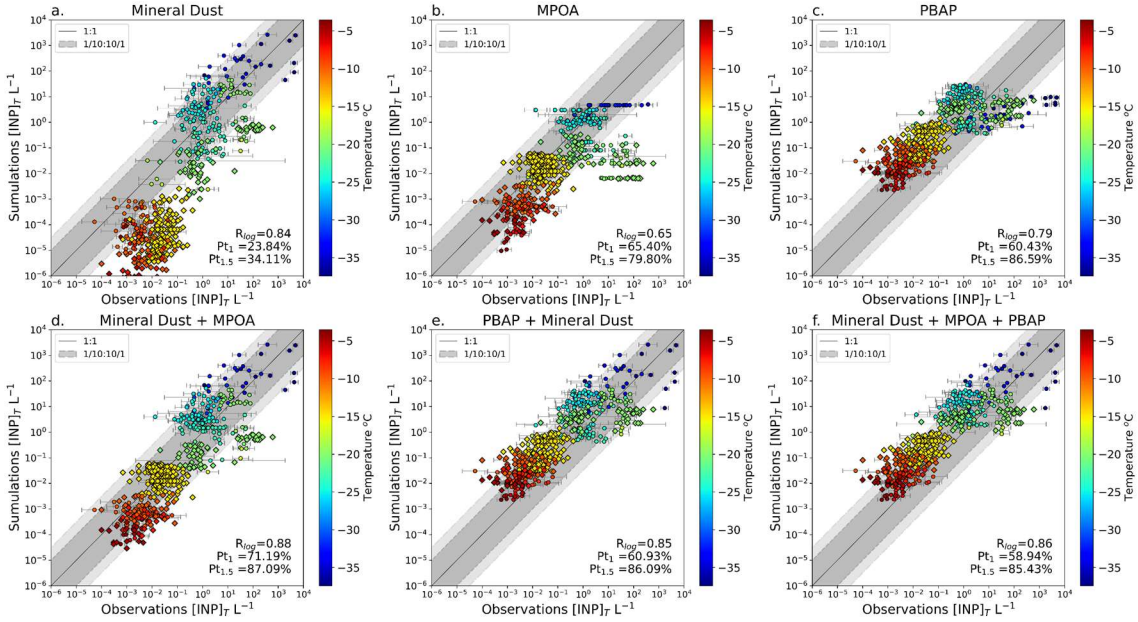

Figure 10: Comparison of INP concentrations calculated at the temperature of the measurements against observations accounting for simulated mineral dust (a), MPOA (b), PBAP (c), mineral dust and MPOA (d), PBAP and mineral dust (e), and mineral dust, MPOA and PBAP (f). The dark grey dashed lines represent

one order of magnitude difference between modelled and observed concentrations, and the light-grey dashed lines depict 1.5 orders of magnitude. The simulated values correspond to monthly mean concentrations, and the error bars correspond to the error of the observed monthly mean INP values. The color bars show the corresponding instrument temperature of the measurement in Celsius (a-f). Pt_1 and $Pt_{1.5}$ are the percentages of data points reproduced by the model within an order of magnitude and 1.5 orders of magnitude, respectively. R is the correlation coefficient, which is calculated with the logarithm of the values. Diamonds correspond to measurements (Bigg, 1990, 1973; Yin et al., 2012) that are compared with the climatological monthly mean simulations. Circles indicate comparisons between temporally and spatially co-located observations and model results.

~~Figures~~

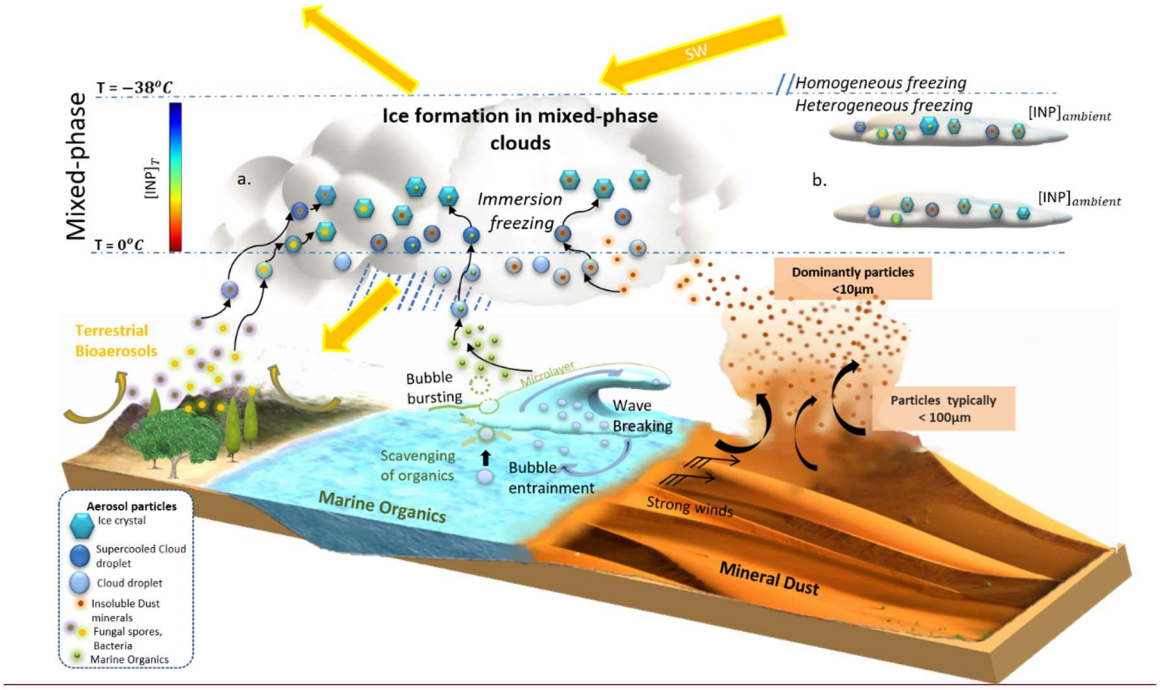

~~Figure 1:~~ ~~Illustration of the formation of INP from mineral dust, MPOA and PBAP, as well as the two ways in which we display INP concentrations in the present study: $[INP]_{ambient}$ calculated at ambient model temperature relevant to non-deep convective mixed-phase clouds using the ambient temperature in the model temperature level (b.), and $[INP]_T$ calculated at a fixed temperature relevant for vertically extended clouds as deep convective systems (a.). The figure is based on Chatziparaschos et al. (2023).~~

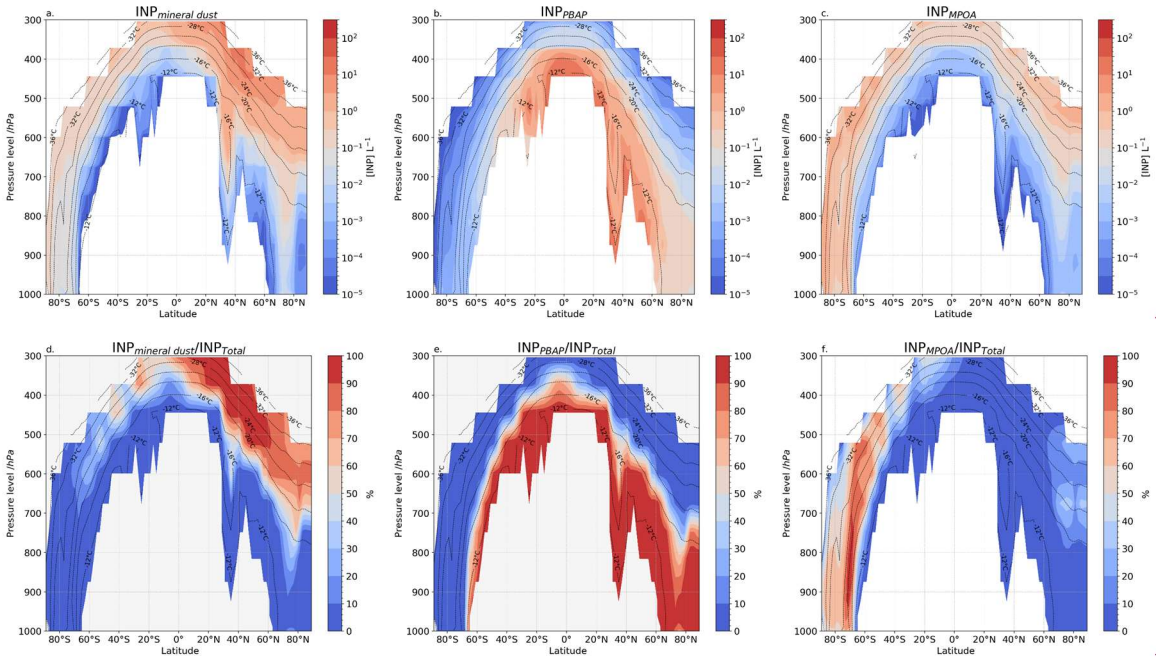

Figure 2: Annual zonal mean profiles of [INP] number concentration calculated by TM4-ECPL for the year 2015 and accounting for (a) mineral dust, (b) fungal spores and bacteria (PBAP) and (c) marine bioaerosols. Panels (d-f) depict the percentage contribution of each species to the total INP concentration. The black contour dashed lines show the annual mean temperature of the model. The colours show (a-c) the INP concentration and (d-f) the percentage contribution of each species to the total INP.

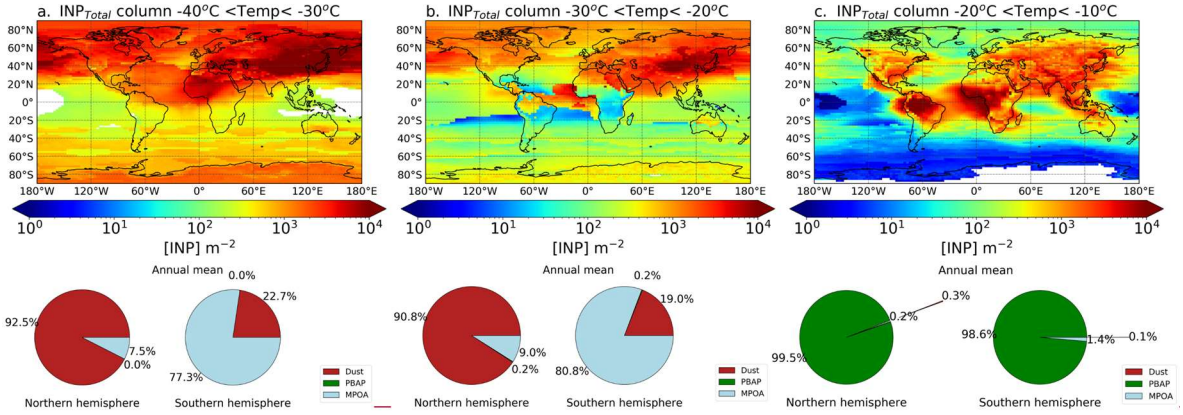

Figure 3: Annual mean INP column concentrations classified by model temperature range between -40 °C to -30 °C (a), -30 °C to -20 °C (b) and -20 °C to -10 °C (c) followed by the respective percentage contributions originated from mineral dust (red), MPOA (light blue) and PBAP (green) in each hemisphere.

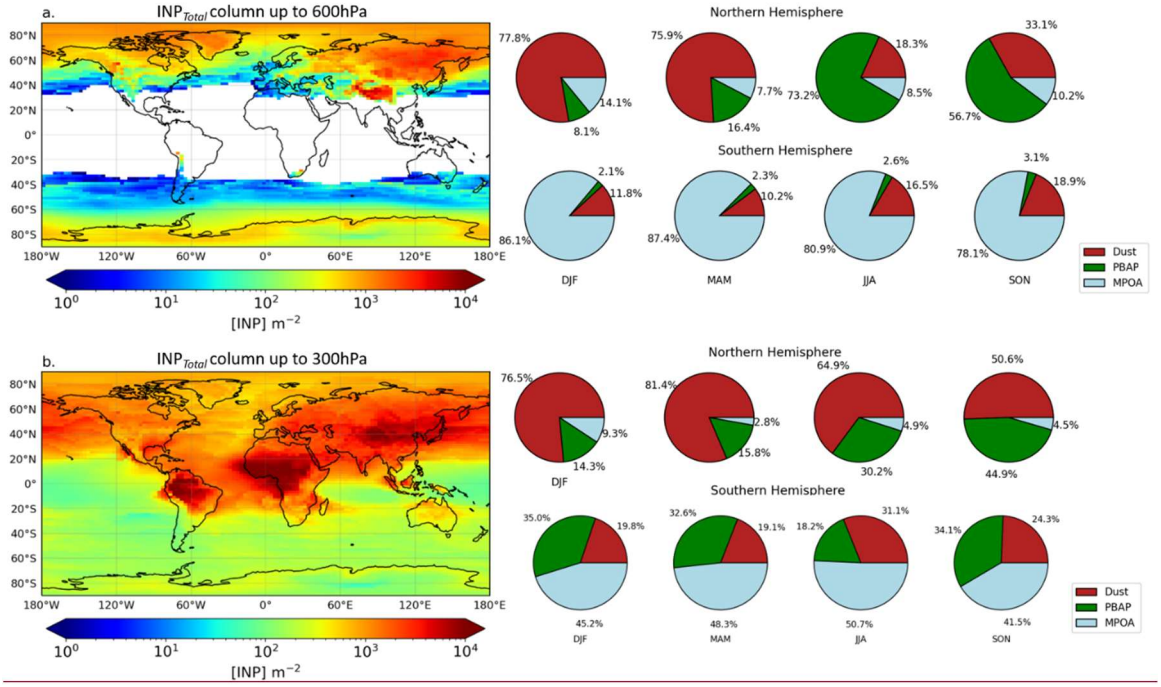

Figure 4: Annual mean INP column concentrations up to 600 hPa (a) and up to 300 hPa (b), and the seasonal percentage contributions originated from mineral dust (red), MPOA (light blue) and PBAP (green) in each hemisphere.

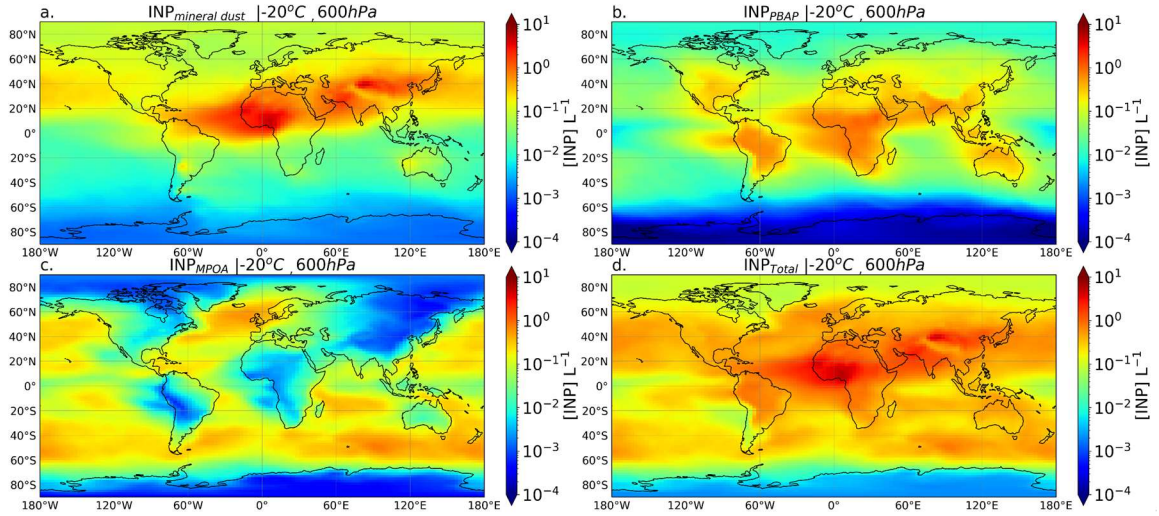

Figure 5. Annual mean distributions calculated by TM4-ECPL for INP number concentrations derived from dust (a), PBAP (b), MPOA (c), and the sum of the aforementioned INP (d) for activation temperature of =20°C, at a pressure level of 600 hPa.

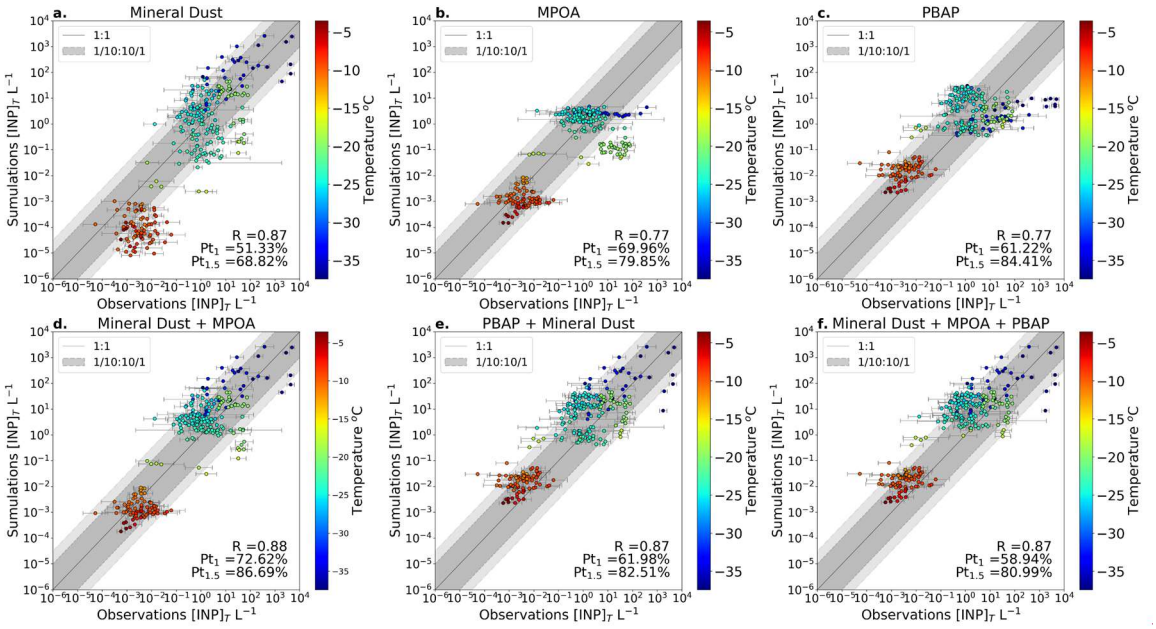

Figure 6. Comparison of INP concentrations calculated at the temperature of the measurements against observations accounting for mineral dust (a), MPOA (b), PBAP (c), mineral dust and MPOA (d), PBAP and mineral dust (e), and mineral dust, MPOA and PBAP (f). The dark grey dashed lines represent one order of magnitude difference between modelled and observed concentrations, and the light grey dashed lines depict 1.5 orders of magnitude. The simulated values correspond to monthly mean concentrations, and the error bars correspond to the error of the observed monthly mean INP values. The color bars show the corresponding instrument temperature of the measurement in Celsius (a–f). Pt1 and Pt1.5 are the percentages of data points reproduced by the model within an order of magnitude and 1.5 orders of magnitude, respectively. R is the correlation coefficient, which is calculated with the logarithm of the values.